# Insight into the prospective evaluation of third-order interelectronic corrections on Li-like ions

R. N. Soguel* and S. Fritzsche

*Theoretisch-Physikalisches Institut, Friedrich-Schiller-Universität Jena, Max-Wien-Platz 1, 07743 Jena, Germany;*
*Helmholtz-Institut Jena, Fröbelstieg 3, 07743 Jena, Germany;*
*and GSI Helmholtzzentrum für Schwerionenforschung GmbH, Planckstraße 1, 64291 Darmstadt, Germany*

(Received 10 May 2023; accepted 8 September 2023; published 12 October 2023)

Relying on the redefined vacuum state approach and based on one-particle three-loop Feynman diagrams, partial third-order interelectronic corrections to the valence electron energy shift are investigated in Li-like ions. The idea is to begin with simple one-particle gauge-invariant subsets composed of Feynman diagrams and to keep track of them in the many-electron frame, which is a strong asset of the formalism. An independent derivation is undertaken with the help of perturbation theory to cross-check the expressions. This two-method scheme helps to resolve how the different terms are distributed among three- and four-electron contributions. Furthermore, it provides a tool to overcome the difficulties related to the derivation of reducible terms, which are tricky to deal with. These two independent derivations and the comparison of the resulting expressions are fully consistent, except for two expressions. In these cases, the discrepancy can be traced back to a different topology of the poles.

DOI: 10.1103/PhysRevA.108.042807

## I. INTRODUCTION

Quantum electrodynamics (QED) is the prototypal gauge theory on which the standard model (SM) of particles relies. Quantum electrodynamics has shown to be impressively reliable in its ability to provide accurate predictions. To illustrate, consider the most precise prediction of the SM, the free-electron magnetic moment in Bohr magnetons, $g/2$. A recent study measured its value to a spectacular precision of 1.3 parts in $10^{13}$ [1]. The SM prediction involves three sectors in its evaluation; it receives contributions from QED, as well as from the hadronic and weak interactions. For the former sector, the asymptotic power series in the fine-structure constant $\alpha$ is expanded up to the fifth order[1] and contains muon and tauon contributions. The bound-electron magnetic moment is more subtle to assess: nevertheless, the stunning accuracy of 5.6 parts in $10^{13}$ [2] was reached. To arrive at this value, a co-trapping of two different isotopes of neon ions was devised. Moreover, pushing QED, in the presence of the binding nuclear field, to its limits is a great way to gain in-depth knowledge about the theory and to probe potentially new physics [3].

Heavy highly charged ions offer a great natural laboratory to study QED in strong-field regimes [4]. Unfortunately, such an experimental high-precision level has not been achieved yet in the transition energies of heavy highly charged ions. Consider as an example the $1s$ Lamb shift in H-like ions, whose experimental value is $460.2 \pm 4.6$ eV [5]. The comparison between theory and experiment allows one to probe first-order QED effects on a 1.7% level [4]. In order to test second-order QED effects, which contribute $-1.26(33)$ eV [6], demanding experimental updates are required [7]. A part of the problem lies in the high energy of the transitions involved, where the sensitivity of the detectors is poor in the KeV regime. Note that a great deal of energy is required to excite the tightest bound electron over the ionization threshold. A way to circumvent this issue is to probe many-electron transition energies, lying from soft x ray to ultraviolet and accessible by laser spectroscopy. Already for He-like ions, the uncertainties drop below the eV level [8,9]. In the case of Li-like ions, the accuracy reached the meV level in both uranium [10,11] and xenon [12] ions. A similar accuracy was achieved in Be-like ions [13]. Also in B-like [14,15], F-like [16,17], and Na-like [18] ions, precise measurements were conducted. To date, the most compelling experimental cases are found to be the $2p_{3/2}$-$2s$ transition in Li-like bismuth ions [19] and the $2p_{1/2}$-$2s$ transition in Li-like uranium ions [11].

The increasing experimental precision drives theoretical predictions to their limits and enforces an accurate description of complex electrons dynamics. The evaluation of the dynamical properties and the structure of highly relativistic, tightly bound electrons in highly charged ions with utmost accuracy represents one of the most important and demanding problems in modern theoretical atomic physics. In this view, the treatment of the interelectronic interaction is a fundament in order to achieve accurate theoretical predictions of the energy levels in many-electron atoms or ions. As a consequence, *ab initio* calculations are the ultimate goal in the quest for many-electron atoms in the frame of bound-state QED (BSQED). The derivations performed so far used a zeroth-order many-electron wave function constructed as a Slater determinant (or sum of Slater determinants) with all electrons involved [20–22]. Such a derivation becomes increasingly difficult to handle for many-electron systems, especially when facing higher-order corrections. The framework

*romain.soguel@uni-jena.de

[1]The authors of Ref. [1] stated that the first four expansion's coefficients $C_i$, $i = 2, 4, 6, 8$, are known exactly, but the last one, $C_{10}$, was required and had to be calculated numerically in order to catch up with the precision of the measurements.

 

of a vacuum state redefinition [23–25] was proposed to tackle third-order interelectronic interactions. Such a technique is not yet widely used in the BSQED community but has already proved helpful in the evaluation of the screened radiative and two-photon exchange corrections to the $g$ factor and hyperfine splitting [26–31], the ground-state and ionization energies of Be-like ions [32,33], respectively, and for the transition energies between low-lying levels [34]. It has been shown to be of intrinsic relevance in the evaluation of the Delbrück scattering above the pair production threshold [35].

This work treats (a partial) third-order interelectronic correction to a single-valence state over closed shells. The aim is to demonstrate that it is feasible to assess third-order interelectronic corrections even though such calculations are especially challenging. To exclude mistakes and as a cross-check of the derived expressions, two different methods are utilized to obtain the results. The first one is an effective one-particle approach, which relies on the redefinition of the vacuum state. It deals with one-particle three-loop diagrams. Its presentation is given in Sec. III, after a brief introduction to BSQED in Sec. II. The idea is to provide a proof of principle that third-order interelectronic corrections can be tackled in the redefined vacuum state framework, owing to the transcription of the one-particle gauge-invariant (GI) subsets to many-electron diagrams. The second method, introduced in Sec. IV, considers a perturbation theory approach to a two-photon-exchange subset. The subset involves a loop contribution, and a potential-like interaction accounts for the perturbation. Then the results are mapped to the three-photon-exchange corrections. This independent derivation of the formulas ensures that potential mistakes are identified and ruled out. The resulting expressions contain infrared (IR) divergences. These are inspected in Sec. V, regularized by the introduction of a photon mass term, and it is shown that they are canceled by terms within the proposed GI subsets. Section VI compares the outcomes of the two methods. The present work ends with a concluding discussion in Sec. VII.

Natural units ($\hbar = c = m_e = 1$) are used throughout this paper and the fine-structure constant is defined as $\alpha = e^2/4\pi$, $e < 0$. Unless explicitly stated otherwise, all integrals are implicitly assumed to be over the full real axis.

## II. BOUND-STATE QED

The relativistic quantum description of the electron-positron field is based on the Dirac equation. The framework of BSQED is based on the resummation of all Feynman diagrams involving the interaction of the (free) electron with the classical field of the nucleus. Such a procedure, applied by Weinberg [36], leads to the bound-state electron propagator. Equivalently, from Furry's perspective [37], the interaction of the electron-positron field with the external classical field of the nucleus can also be taken into account nonperturbatively from the beginning by solving the Dirac equation in the presence of the binding potential,

$$h_{\mathrm{D}}\phi_j(\mathbf{x}) = [-i\boldsymbol{\alpha}\cdot\boldsymbol{\nabla} + \beta + V(\mathbf{x})]\phi_j(\mathbf{x}) = \epsilon_j\phi_j(\mathbf{x}), \tag{1}$$

leading to the so-called Furry picture of QED. Here the $\phi_j(\mathbf{x})$ are the solutions of the stationary Dirac equation in the potential well $V(\mathbf{x})$ occurring due to the nucleus and $j$ stands for all quantum numbers. In addition, $\alpha^k$ and $\beta$ are Dirac matrices and $V(\mathbf{x}) = V_{\mathrm{C}}(\mathbf{x})$ is the external classical Coulomb field arising from the nucleus. Solving Eq. (1) implies an all-order treatment in $\alpha Z$, with $Z$ the nuclear charge, hence going beyond the perturbative regime. The time-dependent solution is the stationary solution $\phi_k(\mathbf{x})$ multiplied by the phase factor $\exp(-i\epsilon_k t)$. For completeness, the extended Furry picture accounts for the presence of a screening potential $U(\mathbf{x})$ besides the Coulomb one, $V(\mathbf{x}) = V_{\mathrm{C}}(\mathbf{x}) + U(\mathbf{x})$, which implies a partial consideration of interelectronic interactions. The redefinition of the vacuum state is conducted in such a way that all core orbitals from the closed shells belong to it [38]. The symbol $|\alpha\rangle$ stands for

$$|\alpha\rangle = a_a^\dagger a_b^\dagger a_c^\dagger \cdots |0\rangle \tag{2}$$

and is referred to as the redefined vacuum state. The following notation is applied, according to Lindgren and Morrison [38] and Johnson [39]: $v$ designates a valence electron, $a, b, c, \ldots$ are core orbitals, and $i, j, k, l, p, \ldots$ correspond to arbitrary states. Upon second quantization, the (noninteracting) electron-positron field can be expanded in terms of creation and annihilation operators. Within the redefined vacuum state approach, such a decomposition still holds but needs to be slightly adapted with respect to the Fermi level $E_\alpha^F$,

$$\psi_\alpha^{(0)}(t,\mathbf{x}) = \sum_{\epsilon_j > E_\alpha^F} a_j\phi_j(\mathbf{x})e^{-i\epsilon_j t} + \sum_{\epsilon_j < E_\alpha^F} b_j^\dagger\phi_j(\mathbf{x})e^{-i\epsilon_j t}. \tag{3}$$

The Fermi level of the redefined vacuum state lies between the highest core state and the valence state, $E_\alpha^F \in (\epsilon_a, \epsilon_v)$. Consequently, the electron propagator is affected in the following manner:

$$\begin{aligned}&\langle\alpha|\, T\left[\psi_\alpha^{(0)}(t,\mathbf{x})\bar{\psi}_\alpha^{(0)}(t',\mathbf{y})\right]|\alpha\rangle \\ &\quad = \frac{i}{2\pi}\int d\omega \sum_j \frac{\phi_j(\mathbf{x})\bar{\phi}_j(\mathbf{y})e^{-i(t-t')\omega}}{\omega - \epsilon_j + i\varepsilon\left(\epsilon_j - E_\alpha^F\right)}.\end{aligned} \tag{4}$$

Here $\epsilon > 0$ implies the limit to zero. It is convenient to define $u = 1 - i\varepsilon$ for later use. The difference between the electron propagator in the redefined vacuum and in the standard one corresponds graphically to a cut of an inner electron line in the Feynman diagram. Such a difference is mathematically implemented via the Sokhotski-Plemelj theorem. For $p \in \mathbb{N}^*$,

$$\begin{aligned}&\sum_j \frac{\phi_j(\boldsymbol{x})\bar{\phi}_j(\mathbf{y})}{\left[\omega - \epsilon_j + i\varepsilon\left(\epsilon_j - E_\alpha^F\right)\right]^p} - \sum_j \frac{\phi_j(\boldsymbol{x})\bar{\phi}_j(\mathbf{y})}{[\omega - \epsilon_j + i\varepsilon(\epsilon_j - E^F)]^p} \\ &\quad = \frac{2\pi i(-1)^p}{(p-1)!}\frac{d^{(p-1)}}{d\omega^{(p-1)}}\sum_a \delta(\omega - \epsilon_a)\phi_a(\boldsymbol{x})\bar{\phi}_a(\mathbf{y}).\end{aligned} \tag{5}$$

This equality is to be understood while integrating in the complex $\omega$ plane. The reader is referred to Refs. [24,25,40] for more details on the vacuum state redefinition within the BSQED framework and the corresponding formalism.

The light-unperturbed normal-ordered Hamiltonian can be expressed as [41]

$$H_0 = \int d^3\mathbf{x}{:}\psi^{(0)\dagger}(t,\mathbf{x})h_{\mathrm{D}}\psi^{(0)}(t,\mathbf{x}){:}. \tag{6}$$

It is left to introduce the light-related part. The interaction Hamiltonian is constructed as

$$H_{\rm int} = \int d^3\mathbf{x}{:}\psi^{(0)\dagger}(t,\mathbf{x})h_{\rm int}\psi^{(0)}(t,\mathbf{x}){:}. \tag{7}$$

It encapsulates the interaction with the quantized electromagnetic field $A_\mu$ and the counterterm associated with the screening potential $-U(\mathbf{x})$, when one works within the extended Furry picture. The explicit expression for $h_{\rm int}$ is $h_{\rm int} = e\alpha^\mu A_\mu(t,\mathbf{x}) - U(\mathbf{x})$. The effect of the interaction Hamiltonian is accounted for within BSQED perturbation theory. Different approaches are possible for its formulation [23,41–43]. The calculation presented in what follows relies on the two-time Green's function (TTGF) method [23].

The photon propagator is denoted by $D_{\mu\nu}(\mathbf{x}-\mathbf{y};\omega)$, with $\omega$ the photon's energy. The interelectronic-interaction operator $I(\mathbf{x}-\mathbf{y};\omega)$ is defined as $I(\mathbf{x}-\mathbf{y};\omega) = e^2\alpha^\mu\alpha^\nu D_{\mu\nu}(\mathbf{x}-\mathbf{y};\omega)$, where $\alpha^\mu = (1,\boldsymbol{\alpha})$. The interelectronic-interaction matrix element $I_{ijkl}(\omega)$ is shorthand for

$$I_{ijkl}(\omega) = \int d^3\mathbf{x}\, d^3\mathbf{y}\, \psi_i^\dagger(\mathbf{x})\psi_j^\dagger(\mathbf{y})I(\mathbf{x}-\mathbf{y};\omega)\psi_k(\mathbf{x})\psi_l(\mathbf{y}) \tag{8}$$

and satisfies the transposition symmetry property $I_{ijkl}(\omega) = I_{jilk}(\omega)$. In the Feynman and Coulomb gauges, the interelectronic-interaction operator $I(\mathbf{x}-\mathbf{y};\omega)$ is an even function of $\omega$.

## III. REDEFINED VACUUM STATE APPROACH

The idea behind a redefinition of the vacuum state is to benefit from a hydrogenlike picture of the problem, the system for which QED is the most developed. This setting is feasible as long as the system under consideration has a single valence electron above some closed shells. The essential notion in introducing a redefined vacuum state is to separate the electron dynamics into the core and valence parts. The first part is relegated to the reference vacuum energy and can be neglected when the transition energy (with a significant many-electron background remaining unchanged) is considered. The key feature of this approach is that the core contributions (arising from the interaction between core electrons, which are canceled in the difference between the excited- and the ground-state energies) are not considered from the very beginning.

The effective one-particle approach, based on a redefinition of the vacuum state, is applied here to more involved Feynman diagrams, as a proof of principle that advanced calculation can be undertaken in this way. The three-photon-exchange corrections investigated, as well as the specific one-particle three-loop Feynman diagrams serving as a starting point of the subsequent consideration, were selected with hindsight. It was necessary to be able to verify, in some manner, the obtained expressions. The perturbative approach requires already known diagrams; therefore, some totally new topology in the considered diagrams was not a realistic choice such as a one-loop correction shared among three electrons exists. Hence, after the introduction of the necessary elements of the TTGF method, a partial recap of the two-photon-exchange correction is undertaken. It both details how the investigated diagrams were selected and serves as a staring point for later developments.

The investigation is carried out for the valence state described as $|v\rangle = a_v^\dagger|\alpha\rangle$ in the perspective of a redefined vacuum state. The cornerstone expression for the energy shift is

$$\Delta E_v = \frac{\frac{1}{2\pi i}\oint_{\Gamma_v} dE(E - \langle v|H_0|v\rangle)\langle v|\Delta g_\alpha(E)|v\rangle}{1 + \frac{1}{2\pi i}\oint_{\Gamma_v} dE\,\langle v|\Delta g_\alpha(E)|v\rangle}, \tag{9}$$

where the contour $\Gamma_v$ is chosen such that it surrounds counterclockwise only the pole $E^{(0)} = \langle v|H_0|v\rangle \equiv \epsilon_v$. Other singularities are kept outside this contour. The Fourier-transformed TTGF matrix element is provided by $\langle v|\Delta g_\alpha(E)|v\rangle = \Delta g_{\alpha,vv}$, where $\Delta g_\alpha(E)$ stands for $\Delta g_\alpha(E) = g_\alpha(E) - g_\alpha^{(0)}(E)$ and $g_\alpha^{(0)}(E)$ is the zeroth-order Fourier-transformed TTGF. The Fourier-transformed TTGF, where the coordinates have been integrated out, is given by

$$g_\alpha(E)\delta(E-E') = \frac{1}{2\pi i}\sum_{i,j}\int d^3x\, d^3y \int dt\, dt' e^{i(Et-E't')}\phi_i^\dagger(\boldsymbol{x})\langle\alpha|T[\psi_\alpha(t,\boldsymbol{x})\psi_\alpha^\dagger(t',\boldsymbol{y})]|\alpha\rangle\,\phi_j(\boldsymbol{y})a_i^\dagger a_j. \tag{10}$$

The treatment of the Green's function within perturbation theory allows one to extend it to the different orders in $\alpha$: $\Delta g_\alpha(E) = \Delta g_\alpha^{(1)}(E) + \Delta g_\alpha^{(2)}(E) + \Delta g_\alpha^{(3)}(E) + \cdots$. Isolating the corresponding third order, the resulting expression for the energy shift can be represented as

$$\begin{aligned}\Delta E_v^{(3)} = {}& \frac{1}{2\pi i}\oint_{\Gamma_v} dE(E-\epsilon_v)\Delta g_{\alpha,vv}^{(3)}(E) - \frac{1}{2\pi i}\oint_{\Gamma_v} dE(E-\epsilon_v)\Delta g_{\alpha,vv}^{(2)}(E)\frac{1}{2\pi i}\oint_{\Gamma_v} dE'\Delta g_{\alpha,vv}^{(1)}(E') \\ & - \frac{1}{2\pi i}\oint_{\Gamma_v} dE(E-\epsilon_v)\Delta g_{\alpha,vv}^{(1)}(E)\left[\frac{1}{2\pi i}\oint_{\Gamma_v} dE'\Delta g_{\alpha,vv}^{(2)}(E') - \left(\frac{1}{2\pi i}\oint_{\Gamma_v} dE'\Delta g_{\alpha,vv}^{(1)}(E')\right)^2\right].\end{aligned} \tag{11}$$

The terms which do not involve $\Delta g_{\alpha,vv}^{(3)}(E)$ are referred to as disconnected elements. Particular attention is required in the treatment of the contributions where the energy of an intermediate state equals the energy of the reference state. These types of contributions are so-called reducible terms.

Three different type of Feynman diagrams are found at this order and are separated accordingly as follows: The one-particle loop diagrams are denoted by (L), the interelectronic-interaction diagrams by (I), and the screened-loop diagrams by (S). This reports focuses on the third-order interelectronic

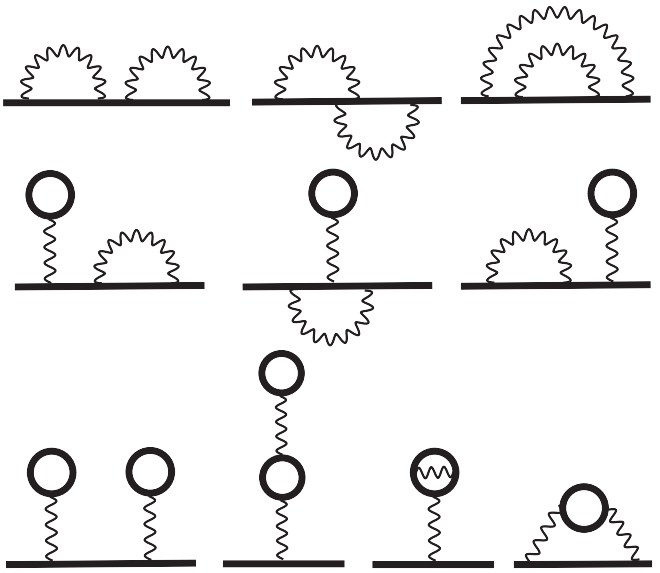

FIG. 1. Second-order one-electron Feynman diagrams labeled as follows: SESE (top row); SEVP (middle row); and VPVP, V(VP)P, V(SE)P, and S(VP)E from left to right in the bottom row. Thick black lines denote the electron propagator in the redefined vacuum state in an external potential $V$. Wavy lines represent the photon propagator.

interactions (3I), also referred to as three-photon-exchange corrections.

### A. Partial recap of two-photon-exchange corrections

To showcase that the vacuum state redefinition approach is working, one resorts to results from Ref. [24]. The two-photon-exchange corrections were derived within the framework of a vacuum state redefinition, thus starting from an effective one-particle picture.

The complete set of second-order one-particle diagrams consists of ten two-loop diagrams. These are presented in Fig. 1. The gauge invariance of the one-particle two-loop diagrams was shown in Ref. [44]. Eight gauge-invariant subsets are identified based on the decomposition provided in this paper. The identified subsets should be gauge invariant in both the redefined and standard vacuum state frameworks. This means that the many-electron diagrams obtained as a difference between redefined and standard vacuum state diagrams can be also classified according to these subsets. The subsets are labeled according to their composition in radiative-loop corrections. In what follows, SE stands for the self-energy loop and VP for the vacuum-polarization loop. The subsets, with the labeling presented in Fig. 1, are the SESE one in the top row, the SEVP one in the middle row, and the VPVP, V(VP)P, V(SE)P, and S(VP)E ones, from left to right, in the bottom row. The eight identified GI subsets in the original Furry picture are, in terms of the one-electron description, SESE (two- and three-electron subsets), SEVP, S(VP)E (two- and three-electron subsets), VPVP, V(VP)P, and V(SE)P.

The resulting two-photon-exchange corrections are divided into three categories, in the many-electron frame: the ladder diagram (referred to as the ladder loop), the crossed-ladder diagram (referred to as the crossed loop), and the three-electron diagram (referred to as the three-electron term in this section). It was shown that that the ladder and crossed loops arose from the SESE and S(VP)E subsets.[2] The SESE subset generates the exchange parts of the two-photon-exchange corrections, whereas the S(VP)E subset generates the direct parts of the two-photon-exchange corrections. The decision was made to pick out the S(VP)E subset as a starting point of the third-order interelectronic corrections. The reasons are (i) its simplicity in terms of the number of diagrams to consider (three vs one) and (ii) that dealing with the exchange part is more difficult. The one-particle three-loop Feynman diagrams are given in Fig. 2 (the S[V(VP)P]E subset) and Fig. 3 [the S(VP)EVP subset]. They correspond to all possible insertions of a VP loop in the S(VP)E graph, being the simplest extension towards a one-loop three-photon-exchange correction. Note that the inclusion of an extra energy-independent interelectronic operator, arising from the cut in the inserted VP loop, does not spoil gauge invariance. The one-photon-exchange operator was shown to be gauge invariant [24]. An important point to highlight is that the $\omega$ flow in the VP loop must be symmetrized in the integrals of the final expressions in order to achieve gauge invariance. It is a crucial step when dealing with the S(VP)E subset (as shown below). The equality (16) and its third-order-pole version were applied to the derived expressions in order to compare them with those based on the perturbation theory approach.

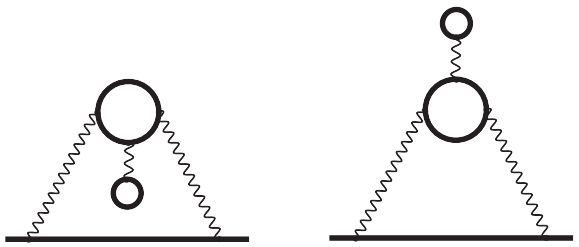

FIG. 2. One-particle three-loop Feynman diagrams of the S[V(VP)P]E subset participating in the third-order contribution to the energy shift of a single-particle state. They are denoted by $H_1$ (left) and $H_2$ (right). The notation is the same as in Fig. 1.

The expressions related to the S(VP)E subset are displayed below, as the initial expressions for later derivations based on perturbation theory. The proof for the gauge invariance of the S(VP)E subset is given numerically, for the Feynman and Coulomb gauges, in Tables I and II at the corresponding lines and analytically in Eq. (B10) for the three-electron terms in

[2]See below Eqs. (54) and (63), respectively, in [24].

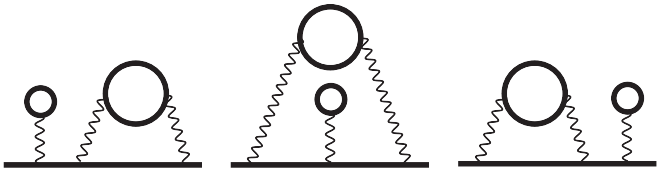

FIG. 3. One-particle three-loop Feynman diagrams of the S(VP)EVP subset participating in the third-order contribution to the energy shift of a single-particle state. They are denoted by $F_1$ (left), $F_2$ (middle), and $F_3$ (right). The notation is similar to Fig. 1.

Ref. [24]. The two-electron irreducible part $\Delta E_v^{(2I)S(VP)E,2e,irr}$ reads

$$\Delta E_v^{(2I)S(VP)E,2e,irr} = \frac{i}{2\pi}\int d\omega\left(\sum_{a,i,j}{}' \frac{I_{vjia}(\omega)I_{iavj}(\omega)}{(\epsilon_v-\omega-\epsilon_i u)(\epsilon_a-\omega-\epsilon_j u)} + \sum_{a,i,j}^{(i,j)\neq(a,v)} \frac{I_{vaij}(\omega)I_{ijva}(\omega)}{(\epsilon_v-\omega-\epsilon_i u)(\epsilon_a+\omega-\epsilon_j u)}\right), \quad (12)$$

where one excludes the contribution with $\epsilon_i=\epsilon_v$ and $\epsilon_j=\epsilon_a$ from the crossed-direct term (first item) by hand and denotes this by the prime on the sum. The two-electron reducible part $\Delta E_v^{(2I)S(VP)E,2e,red}$, coming from the ladder-direct restriction $\epsilon_i+\epsilon_j=\epsilon_a+\epsilon_v$ together with the excluded part from the irreducible crossed-direct term, yields

$$\Delta E_v^{(2I)S(VP)E,2e,red} = -\frac{i}{4\pi}\int d\omega\left(\frac{1}{(\omega+i\varepsilon)^2}+\frac{1}{(-\omega+i\varepsilon)^2}\right) \times \sum_{a,a_1,v_1} I_{vaa_1v_1}(\Delta_{va}-\omega)I_{a_1v_1va}(\Delta_{va}-\omega). \quad (13)$$

The three-electron irreducible part $\Delta E_v^{(2I)S(VP)E,3e,irr}$ yields

$$\Delta E_v^{(2I)S(VP)E,3e,irr} = -\sum_{a,b,i}^{(i,b)\neq(v,a)} \frac{I_{vabi}(\Delta_{vb})I_{biva}(\Delta_{vb})+I_{vaib}(\Delta_{ba})I_{ibva}(\Delta_{ba})}{(\epsilon_v+\epsilon_a-\epsilon_b-\epsilon_i)} - \sum_{a,b,i}\frac{I_{viba}(\Delta_{vb})I_{bavi}(\Delta_{vb})}{(\epsilon_a+\epsilon_b-\epsilon_v-\epsilon_i)}, \quad (14)$$

together with the corresponding reducible part

$$\Delta E_v^{(2I)S(VP)E,3e,red} = -\sum_{a,a_1,v_1} I_{vaa_1v_1}(\Delta_{va})I'_{a_1v_1va}(\Delta_{va}). \quad (15)$$

As a side remark, note that the identity

$$\frac{-1}{(x+i\varepsilon)^2}+\frac{1}{(-x+i\varepsilon)^2}=\frac{2\pi}{i}\partial_x\delta(x) \quad (16)$$

was used to symmetrize the $\omega$ flow in the VP loop or, in other words, to symmetrize the pole structure with respect to the real-line axis.

### B. The S[V(VP)P]E subset

The Green's function corresponding to each diagram in the subset is given by

$$\Delta g^{(3)H_1}_{\alpha,vv}(E) = \frac{1}{(E-\epsilon_v)^2}\left(\frac{i}{2\pi}\right)^3\sum_{i,j,k,l,p}\int d\omega\, dk_1 dk_2 \frac{I_{vpik}(\omega)}{\left[E-\omega-\epsilon_i+i\varepsilon\left(\epsilon_i-E^F_\alpha\right)\right]\left[k_1-\epsilon_j+i\varepsilon\left(\epsilon_j-E^F_\alpha\right)\right]} \times \frac{I_{kjlj}(0)I_{lipv}(\omega)}{\left[k_2-\epsilon_k+i\varepsilon\left(\epsilon_k-E^F_\alpha\right)\right]\left[k_2-\epsilon_l+i\varepsilon\left(\epsilon_l-E^F_\alpha\right)\right]\left[k_2-\omega-\epsilon_p+i\varepsilon\left(\epsilon_p-E^F_\alpha\right)\right]} \quad (17)$$

for $H_1$ and by

$$\Delta g^{(3)H_2}_{\alpha,vv}(E) = \frac{1}{(E-\epsilon_v)^2}\left(\frac{i}{2\pi}\right)^3\sum_{i,j,k,l,p}\int d\omega\, dk_1 dk_2 \frac{I_{vkij}(\omega)}{\left[E-\omega-\epsilon_i+i\varepsilon\left(\epsilon_i-E^F_\alpha\right)\right]\left[k_1-\epsilon_j+i\varepsilon\left(\epsilon_j-E^F_\alpha\right)\right]} \times \frac{I_{lpkp}(0)I_{jilv}(\omega)}{\left[k_1-\omega-\epsilon_k+i\varepsilon\left(\epsilon_k-E^F_\alpha\right)\right]\left[k_1-\omega-\epsilon_l+i\varepsilon\left(\epsilon_l-E^F_\alpha\right)\right]\left[k_2-\epsilon_p+i\varepsilon\left(\epsilon_p-E^F_\alpha\right)\right]} \quad (18)$$

for $H_2$. According to the line of reasoning presented in the treatment of the SESE subset in Ref. [24], starting from the previous Green's functions, the extraction of the different three-photon-exchange corrections is carried out with the subtraction of the corresponding expression in the standard vacuum state

$$\Delta E_v^{(3)} - \Delta E_v^{(3L)} = \Delta E_v^{(3I)} + \Delta E_v^{(3S)}. \quad (19)$$

In other words, within the framework of a redefined vacuum state, the interelectronic and the screened corrections are treated on the same footing. As the diagrams are one-particle irreducible (1PI), one does not need to worry about the disconnected elements in Eq. (11). Note that double cuts are possible in both diagrams, leading to so-called nondiagrammatic elements. These are important to consider in order to properly treat the reducible part. Nondiagrammatic elements are expressions that cannot be drawn as single Feynman diagrams since they involve reducible parts. The results are separated in three- and four-electron contributions.

To illustrate the extraction procedure based on Eq. (19), the term-by-term three-electron (loop diagram) expressions obtained afterward are displayed explicitly below for $H_1$. One distinguishes between three different type of terms: irreducible (irr), reducible 1 (red1), and reducible 2 (red2). The irreducible terms correspond to a first-order pole ($S$-matrix terms) in the first term on the right-hand side, namely the one with $\Delta g^{(3)}$ of Eq. (11), whereas the reducible 1 and 2 terms correspond to second- and third-order poles, respectively, in the first term on the right-hand side, namely the one with $\Delta g^{(3)}$ of Eq. (11). To keep track of the source of generated reducible parts, a subscript is used with the previous notation,

for example, $v_1$, $a_1$, and $b_2$, where $\epsilon_{i_1} = \epsilon_i$. The different terms corresponding to crossed graphs are found to be

$$\Delta E_{v,H_1}^{(3I)3e,cross,irr} = \frac{i}{2\pi}\int d\omega \sum_{i,j,k}^{k\neq b} \frac{I_{vjib}(\omega) I_{baka}(0) I_{kijv}(\omega)}{(\epsilon_v - \omega - \epsilon_i u)(\epsilon_b - \omega - \epsilon_j u)(\epsilon_b - \epsilon_k u)}, \tag{20}$$

$$\Delta E_{v,H_1}^{(3I)3e,cross,irr} = \frac{i}{2\pi}\int d\omega \sum_{i,j,k}^{k\neq b} \frac{I_{vjik}(\omega) I_{kaba}(0) I_{bijv}(\omega)}{(\epsilon_v - \omega - \epsilon_i u)(\epsilon_b - \omega - \epsilon_j u)(\epsilon_b - \epsilon_k u)}. \tag{21}$$

The terms associated with ladder graphs are given as

$$\Delta E_{v,H_1}^{(3I)3e,lad,irr} = \frac{i}{2\pi}\int d\omega \sum_{i,j,k}^{\{i,j\}\neq\{v,b\},\{i,k\}\neq\{v,b\}} \frac{I_{vbij}(\omega) I_{jaka}(0) I_{kibv}(\omega)}{(\epsilon_v - \omega - \epsilon_i u)(\epsilon_b + \omega - \epsilon_j u)(\epsilon_b + \omega - \epsilon_k u)}, \tag{22}$$

$$\Delta E_{v,H_1}^{(3I)3e,lad,red1} = -\frac{i}{2\pi}\int d\omega \sum_{i,j,k}^{\{i,j\}=\{v,b\},\{i,k\}\neq\{v,b\}} \frac{I_{vbij}(\omega) I_{jaka}(0) I_{kibv}(\omega)}{(\epsilon_v - \omega - \epsilon_i u)^2(\epsilon_b + \omega - \epsilon_k u)}, \tag{23}$$

$$\Delta E_{v,H_1}^{(3I)3e,lad,red1} = -\frac{i}{2\pi}\int d\omega \sum_{i,j,k}^{\{i,j\}\neq\{v,b\},\{i,k\}=\{v,b\}} \frac{I_{vbij}(\omega) I_{jaka}(0) I_{kibv}(\omega)}{(\epsilon_v - \omega - \epsilon_i u)^2(\epsilon_b + \omega - \epsilon_j u)}, \tag{24}$$

$$\Delta E_{v,H_1}^{(3I)3e,lad,red2} = \frac{i}{2\pi}\int d\omega \sum_{i,j,k}^{\{i,j\}=\{v,b\},\{i,k\}=\{v,b\}} \frac{I_{vbij}(\omega) I_{jaka}(0) I_{kibv}(\omega)}{(\epsilon_v - \omega - \epsilon_i u)^3}. \tag{25}$$

The nondiagrammatic element for $H_1$ reads

$$\Delta E_{v,H_1}^{(3I)3e,cross,red1} = -\frac{i}{2\pi}\int d\omega \sum_{i,j} \frac{I_{vjib}(\omega) I_{bab_1a}(0) I_{b_1ijv}(\omega)}{(\epsilon_v - \omega - \epsilon_i u)(\epsilon_b - \omega - \epsilon_j u)^2}. \tag{26}$$

The expressions presented above are the bare results after carrying out the difference of the vacuum states to extract the interelectronic interactions. We emphasize that the reducible expressions are IR divergent. These IR divergences are extracted and regularized later on, such as the symmetrization of the poles with regard to the real axis. The term-by-term interelectronic expressions related to $H_2$ are given in Appendix A. They are needed to show the explicit cancellation of IR divergences at the single Feynman diagram level. The final interelectronic three-electron expressions are found in Appendix C, when the comparison with the results obtained from the perturbation theory approach is made. The four-electron terms are displayed in Appendix D, again for a comparison with the outcome of the second method.

### C. The S(VP)EVP subset

As a second example, consider the Green's function associated with the $F_2$ diagram

$$\Delta g_{\alpha,vv}^{(3)F_2}(E) = \frac{1}{(E-\epsilon_v)^2}\left(\frac{i}{2\pi}\right)^3 \sum_{i,j,k,l,p}\int d\omega dk_1 dk_2 \frac{I_{vlil}(\omega)}{\left[E-\omega-\epsilon_i+i\varepsilon\left(\epsilon_p - E_\alpha^F\right)\right]\left[k_1-\epsilon_j+i\varepsilon\left(\epsilon_j - E_\alpha^F\right)\right]} \times \frac{I_{ijkj}(0) I_{lkpv}(\omega)}{\left[E-\omega-\epsilon_k+i\varepsilon\left(\epsilon_p - E_\alpha^F\right)\right]\left[k_2-\epsilon_l+i\varepsilon\left(\epsilon_l - E_\alpha^F\right)\right]\left[k_2-\omega-\epsilon_p+i\varepsilon\left(\epsilon_p - E_\alpha^F\right)\right]}. \tag{27}$$

The identical procedure as stated above is applied to infer the three-photon-exchange corrections. The diagrams are not 1PI, with the exception of $F_2$. Therefore, one has to consider the second-order Green's function $\Delta g_\alpha^{(2)S(VP)E}$ and the first-order one $\Delta g_\alpha^{(1)VP}$ to evaluate the disconnected elements in Eq. (11). It turns out that only the first term in the square bracket of the second line survives. The disconnected elements are important to account for as they remove the redundancies in the reducible parts. To illustrate, $F_1$ and $F_3$ give redundant reducible terms, but the disconnected elements remove the extra ones, coming from $F_1$ in this case. A small subtlety is nevertheless present if an extra pole is explicitly extracted. In such a case, this reducible term is kept for two reasons: first, because it cannot be generated in the disconnected ones, and second, which is more important, to achieve the IR finiteness of the expressions in the subset. Hence, for the S(VP)EVP subset, on the top of the peculiar extra pole term arising from $F_1$, only the $F_2$ and $F_3$ reducible IR divergent expressions are displayed in Table I. Nondiagrammatic elements are only present in the $F_2$ diagram and are of four-electron type. The results are separated in three- and four-electron contributions. The Feynman diagram $F_2$ leads to the subsequent expressions.

Only an expression associated with a crossed-loop graph is found,

$$\Delta E^{(3I)3e,cross}_{v,F_2} = \frac{i}{2\pi}\int d\omega \sum_{i,j,k} \frac{I_{vkib}(\omega) I_{iaja}(0) I_{bjkv}(\omega)}{(\epsilon_v - \omega - \epsilon_i u)(\epsilon_v - \omega - \epsilon_j u)(\epsilon_b - \omega - \epsilon_k u)}, \tag{28}$$

so it is for the ladder-loop graph, but incorporating the different types of terms (irr, red1, and red2) stated above,

$$\Delta E^{(3I)3e,lad,irr}_{v,F_2} = \frac{i}{2\pi}\int d\omega \sum_{i,j,k}^{\{i,k\}\neq\{v,b\},\{j,k\}\neq\{v,b\}} \frac{I_{vbik}(\omega) I_{iaja}(0) I_{kjbv}(\omega)}{(\epsilon_v - \omega - \epsilon_i u)(\epsilon_v - \omega - \epsilon_j u)(\epsilon_b + \omega - \epsilon_k u)}, \tag{29}$$

$$\Delta E^{(3I)3e,lad,red1}_{v,F_2} = -\frac{i}{2\pi}\int d\omega \sum_{i,j,k}^{\{i,k\}=\{v,b\},\{j,k\}\neq\{v,b\}} \left[\frac{I_{vbik}(\omega) I_{iaja}(0) I_{kjbv}(\omega)}{(\epsilon_v - \omega - \epsilon_i u)^2}\left(\frac{1}{(\epsilon_v - \omega - \epsilon_i u)} + \frac{1}{(\epsilon_b + \omega - \epsilon_k u)}\right) + \frac{I_{vbik}(\omega) I_{iaja}(0) I_{kjbv}(\omega)}{(\epsilon_v - \omega - \epsilon_i u)^2(\epsilon_v - \omega - \epsilon_j u)}\right], \tag{30}$$

$$\Delta E^{(3I)3e,lad,red1}_{v,F_2} = -\frac{i}{2\pi}\int d\omega \sum_{i,j,k}^{\{i,k\}\neq\{v,b\},\{j,k\}=\{v,b\}} \left[\frac{I_{vbik}(\omega) I_{iaja}(0) I_{kjbv}(\omega)}{(\epsilon_v - \omega - \epsilon_i u)^2}\left(\frac{1}{(\epsilon_v - \omega - \epsilon_j u)} + \frac{1}{(\epsilon_b + \omega - \epsilon_k u)}\right) + \frac{I_{vbik}(\omega) I_{iaja}(0) I_{kjbv}(\omega)}{(\epsilon_v - \omega - \epsilon_i u)(\epsilon_v - \omega - \epsilon_j u)^2}\right], \tag{31}$$

$$\Delta E^{(3I)3e,lad,red2}_{v,F_2} = \frac{i}{2\pi}\int d\omega \sum_{i,j,k}^{\{i,k\}=\{v,b\},\{j,k\}=\{v,b\}} \left[-\frac{I_{vbik}(\omega) I_{iaja}(0) I_{kjbv}(\omega)}{(\epsilon_v - \omega - \epsilon_i u)(\epsilon_v - \omega - \epsilon_j u)}\left(\frac{1}{(\epsilon_v - \omega - \epsilon_i u)} + \frac{1}{(\epsilon_v - \omega - \epsilon_j u)}\right) + \frac{I_{vbik}(\omega) I_{iaja}(0) I_{kjbv}(\omega)}{(\epsilon_v - \omega - \epsilon_i u)^3}\right]. \tag{32}$$

As in the case of the S[V(VP)P]E subset, the expressions shown above are those obtained in the extraction procedure of the interelectronic interaction, as the difference of the vacuum states. More work is required to extract the IR divergences of the reducible terms, to regularize them, as well as to symmetrize the poles with regard to the real axis. The expressions associated with $F_1$ and $F_3$ diagrams are found in Appendix B. The explicit cancellation of IR divergences at the single diagram level requires them. The final expressions associated with the one-loop three-photon-exchange diagrams are found in Appendix C, when comparing with the results from the second derivation. The four-electron terms are displayed, for a comparison with the perturbation theory approach, in Appendix D.

## IV. PERTURBATION THEORY APPROACH

The idea behind this approach is to perturb a two-photon-exchange correction by the presence of some potential-like interaction $\mathcal{V}$, to its first order. This method was applied in Ref. [45] to generate the two-photon-exchange corrections to the $g$ factor of Li-like ions. Specifically, the one-electron external wave function is perturbed as

$$|i\rangle \to |i\rangle + |\delta i\rangle\,, \quad |\delta i\rangle = \sum_{j\neq i} \frac{|j\rangle\,\mathcal{V}_{ji}}{\epsilon_i - \epsilon_j}, \tag{33}$$

and the energy accordingly to

$$\epsilon_i \to \epsilon_i + \delta\epsilon_i, \quad \delta\epsilon_i = \mathcal{V}_{ii}, \tag{34}$$

leading to the perturbation in the argument of the interelectronic operator

$$I(\Delta_{va}) \to I(\Delta_{va} + \delta\Delta_{va}) \approx I(\Delta_{va}) + I'(\Delta_{va})(\delta\epsilon_v - \delta\epsilon_a). \tag{35}$$

The $\Delta_{va}$ stands for $\Delta_{va} = \epsilon_v - \epsilon_a$. The electron propagator (4) involved in the loops has to be perturbed as well. In its energy-position representation, one finds

$$\begin{aligned} S_{\delta\mathcal{V}}(\epsilon_k \pm \omega; \mathbf{x}, \mathbf{y}) &= \delta_{\mathcal{V}}\left(\sum_i \frac{|i\rangle\langle i|}{\epsilon_k \pm \omega - \epsilon_i u}\right) \\ &= \sum_{i,j} \frac{|i\rangle\,\mathcal{V}_{ij}\,\langle j|}{(\epsilon_k \pm \omega - \epsilon_i u)(\epsilon_k \pm \omega - \epsilon_j u)} \\ &\quad - \sum_i \frac{|i\rangle\,\mathcal{V}_{kk}\,\langle i|}{(\epsilon_k \pm \omega - \epsilon_i u)^2}. \end{aligned} \tag{36}$$

It is a slight generalization of the propagator found in Ref. [46]. This expression is also valid when $\omega = 0$, namely, for the four-electron case. However, one should distinguish when to use each of the two terms. If both terms in parentheses $(\epsilon_k \pm \omega - \epsilon_{i,j} u)|_{\omega=0}$ are nonzero, then the first piece of the perturbed propagator is to be used. If one of the terms in parentheses $(\epsilon_k \pm \omega - \epsilon_{i,j} u)|_{\omega=0}$ is zero, then the second piece of the perturbed propagator is to be used, with the appropriate index. In such a way, the operator $\Xi$ of Eq. (46) in Ref. [45] is reproduced.

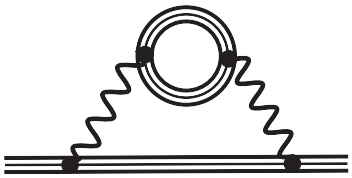

FIG. 4. One-particle two-loop Feynman diagram corresponding to the perturbed S(VP)P subset in the redefined vacuum state formalism in an external potential $V$. The triple line indicates the electron propagator perturbed by the potential-like interaction $\mathcal{V}$. The notation is similar to Fig. 2.

In the end, one trades the potential-link interaction matrix element for a one-photon-exchange one,

$$\mathcal{V}_{ij} \to I_{iaja}(0), \tag{37}$$

to match the three-photon-exchange formulas. Let us pause to comment on the last step presented above. A link between the potential-like interaction and the one-photon-exchange interaction is drawn. The logic goes as follows. Consider, for example, the Wichmann-Kroll potential [47]. It accounts for an all-order treatment, in $\alpha Z$, of the interaction of the free-electron vacuum-polarization loop (first order in $\alpha$) with the Coulomb potential.[3] [As a side comment, the Uehling potential [53], which takes into account the electric polarization of the vacuum (state), is the lowest-order approximation (in $\alpha Z$) of the vacuum-polarization loop within the Coulomb field of the nucleus. One usually considers that the Wichmann-Kroll potential does not take the Uehling potential into account.] Although the Wichmann-Kroll potential is such a potential-like interaction, it deals with the full Green's function. However, the potential-like interaction considered above incorporates only the core electrons. Therefore, going half a step back, one can imagine having an all-order $\alpha Z$ Wichmann-Kroll-like potential mapped to the vacuum-polarization loop only for the core electrons. The inner structure of the vacuum-polarization potential-like interaction is then unraveled by a cut in the loop. Hence, one can think of the potential-like interaction as an effective one-electron operator but implicitly accounting for a corrected wave function or representing a screened correction.

Thus, one perturbs the S(VP)E equations (12)–(15) according to Eqs. (33)–(36) and finds the desired formulas under the replacement (37). The Feynman diagram corresponding to the $\mathcal{V}$-perturbed S(VP)E subset is displayed in Fig. 4. The triple-line notation represents the electron propagator perturbed by the potential-like interaction $\mathcal{V}$. It was shown that the two-electron subset and the three-electron subset are separately gauge invariant [24]. The perturbation is initially a potential-like interaction $\mathcal{V}$, turned into a one-photon-exchange operator in the vanishing energy limit, which is gauge independent too. Therefore, it should be well founded to expect that the results derived from this approach also fulfill the requirement of gauge invariance, namely, on the three- and four-electron levels, respectively. The open question is whether the separation into S(VP)EVP and S[V(VP)P]E subsets holds also at the three- and four-electron levels, as it is thought to be the case. Hence, starting from the $\mathcal{V}$-perturbed S(VP)E GI expressions, one should be able to disentangle the various terms found via the redefinition of the vacuum state approach and assign them to either the three- or the four-electron contribution. The results relying on this method are displayed in Appendix C for the former case and in Appendix D for the latter.

[3]A potential which accounts for a partial two-loop (second order in $\alpha$) VP correction is the Kallen-Sabry potential [48–52].

## V. REGULARIZATION OF INFRARED DIVERGENCES

Infrared divergences occur when the energy flowing through the loop ($\omega$) leads to a vanishing denominator of the electron propagator at $\omega \to 0$. At the level of two-photon-exchange corrections, this behavior was only met in ladder reducible expressions, where the removal of some terms in the summation of the crossed expressions was carried out to cancel IR divergent parts of the ladder reducible terms [54]. In the case of the three-photon-exchange corrections, it can also arise from crossed reducible expressions. The analysis of IR divergences is conducted in the Feynman gauge, but the resulting pairing of the expressions is valid generally by virtue of gauge invariance. According to Shabaev [23], one introduces the following integral representation for the complex-exponential term of the photon propagator, including a photon mass term $\mu$:

$$e^{i\sqrt{\omega^2-\mu^2+i\varepsilon}|\mathbf{x}-\mathbf{y}|} = \frac{-2}{\pi}\int_0^\infty dk \frac{k\sin(k|\mathbf{x}-\mathbf{y}|)}{\omega^2-k^2-\mu^2+i\varepsilon}. \tag{38}$$

The photon mass plays the role of an energy cutoff (IR regulator). Notice that the condition on the branch of the square root is changed to $\mathrm{Im}(\sqrt{\omega^2-\mu^2+i\varepsilon}) > 0$. In the rest of the section, the use of $r_{12} \equiv |\mathbf{x}-\mathbf{y}|$ is preferred. Such a type of integral is met when facing IR divergences

$$\mathcal{I}_{n,m_\pm,p} \equiv \frac{-i}{2\pi}\int d\omega \frac{I(\omega)I(\omega)I(0)}{(-\omega+i\varepsilon)^n(\Delta\pm\omega+i\varepsilon)^m\tilde{\Delta}^p}, \tag{39}$$

with $n = 1, 2, 3$; $m = 0, 1$; $p = 0, 1$; and the constraint $n + m + p = 3$. The plus sign stands for the IR divergent ladder reducible terms and the minus sign for the compensating crossed terms. Calculations are performed by the application of the integral 3.773(3) [or 3.729(2)] in Ref. [55]. The first step is to show that for a first-order pole $n = 1$, the result is IR finite. There is no necessity to introduce a photon mass or to use the integral representation of the complex exponential. It is sufficient to Wick rotate the integration contour with the substitution $\omega = i\omega_E$. Afterward, the principal value of the integral, denoted by $\mathcal{P}$, is considered. One starts with the simplest case

$$\mathcal{I}_{1,0,2} = \frac{I(0)}{2\pi\tilde{\Delta}^2}\mathcal{P}\int_0^{i\infty} d\omega_E \frac{I(-i\omega_E)I(-i\omega_E) - I(i\omega_E)I(i\omega_E)}{i\omega_E} - \frac{i}{2\tilde{\Delta}^2}I(0)I(0)I(0). \tag{40}$$

The integral term reads explicitly

$$\frac{\alpha^2}{r_{12}r_{34}}\alpha_{1\mu}\alpha_2^\mu\alpha_{3\nu}\alpha_4^\nu\mathcal{P}\int_0^{i\infty} d\omega_E \frac{e^{-\omega_E R} - e^{\omega_E R}}{i\omega_E}, \tag{41}$$

giving a finite contribution in the limit $\omega \to 0$. Here $R$ stands for $R = r_{12} + r_{34}$. One sees that the real part is IR finite; the imaginary one is as well in this simple example. The second case $\mathcal{I}_{1,2_-,0}$ requires one more step, a partial fraction decomposition, so that the Cauchy principal value can be applied (recall that the principal value picks only the residues, hence no contribution from second- or higher-order poles):

$$\mathcal{I}_{1,2_-,0} = \frac{I(0)}{2\pi\Delta^2}\mathcal{P}\int_0^{i\infty} d\omega_E \left(\frac{I(-i\omega_E)I(-i\omega_E) - I(i\omega_E)I(i\omega_E)}{i\omega_E} - \frac{I(-i\omega_E)I(-i\omega_E)}{\Delta + i\omega_E} - \frac{I(i\omega_E)I(i\omega_E)}{\Delta - i\omega_E}\right) - \frac{i}{\Delta^2} I(0)[I(0)I(0) - I(\Delta)I(\Delta)]. \tag{42}$$

The first integrand was shown to be IR finite just above. For the remaining two integrands, it is clear that $\Delta$ plays the role of an IR cutoff, preventing the expression from diverging in the limit $\omega \to 0$. The case $\mathcal{I}_{1,1_-,1}$ is not met in the diagrams under consideration and is therefore not assessed. Let us discuss the IR divergences arising from second-order poles. The first case $\mathcal{I}_{2,0,1}$ considers the insertion of the interelectronic operator on the external leg of a one-loop diagram. One has

$$\mathcal{I}_{2,0,1} = \frac{-\alpha^3 R}{\pi r_{12} r_{34} r_{56} \tilde{\Delta}} \alpha_{1\mu}\alpha_2^\mu \alpha_{3\nu}\alpha_4^\nu \alpha_{5\rho}\alpha_6^\rho K_0(\mu R) \approx \frac{-\alpha^3 R}{\pi r_{12} r_{34} r_{56} \tilde{\Delta}} \alpha_{1\mu}\alpha_2^\mu \alpha_{3\nu}\alpha_4^\nu \alpha_{5\rho}\alpha_6^\rho \left(\ln\frac{\mu}{2} + \gamma + \ln R\right) \tag{43}$$

in the limit $\mu \to 0$. The $K_n(x)$ are imaginary Bessel functions of the second kind. The IR logarithmic divergent behavior identical to that in the two-photon-exchange ladder reducible case is recovered [23]. The corresponding crossed diagram cancels the IR divergent term, leaving a well-behaved expression. The second case $\mathcal{I}_{2,1_+,0}$ is when the interelectronic operator is inserted within the electron propagator of the loop in the diagram. One faces

$$\mathcal{I}_{2,1_+,0} = \frac{\alpha^3}{\pi r_{12} r_{34} r_{56}} \alpha_{1\mu}\alpha_2^\mu \alpha_{3\nu}\alpha_4^\nu \alpha_{5\rho}\alpha_6^\rho \int_0^\infty dk\, k \sin(kR) \left(\frac{1}{(k^2+\mu^2)^{3/2}(\Delta - \sqrt{k^2+\mu^2})} - \frac{2}{(k^2+\mu^2)\Delta^2}\right). \tag{44}$$

This IR divergence is compensated by a similar crossed graph, represented by the integral $\mathcal{I}_{2,1_-,0}$ where the interelectronic operator is also inserted within the electron propagator of the loop

$$\mathcal{I}_{2,1_-,0} = \frac{-\alpha^3}{\pi r_{12} r_{34} r_{56}} \alpha_{1\mu}\alpha_2^\mu \alpha_{3\nu}\alpha_4^\nu \alpha_{5\rho}\alpha_6^\rho \int_0^\infty dk\, k \sin(kR) \times \left(\frac{-1}{(k^2+\mu^2)^{3/2}(\Delta + \sqrt{k^2+\mu^2})} + \frac{2}{(k^2+\mu^2-\Delta^2)\Delta^2} - \frac{2}{(k^2+\mu^2)\Delta^2}\right). \tag{45}$$

However, the cancellation is not straightforward at this step. A partial fraction decomposition allows one to greatly simplify the previous expressions, when they are added together:

$$\mathcal{I}_{2,1_-,0} + \mathcal{I}_{2,1_+,0} = \frac{-2\alpha^3}{\pi r_{12} r_{34} r_{56} \Delta^2} \alpha_{1\mu}\alpha_2^\mu \alpha_{3\nu}\alpha_4^\nu \alpha_{5\rho}\alpha_6^\rho \int_0^\infty dk \frac{k\sin(kR)}{k^2+\mu^2} = \frac{-2\alpha^3}{\pi r_{12} r_{34} r_{56} \Delta^2} \alpha_{1\mu}\alpha_2^\mu \alpha_{3\nu}\alpha_4^\nu \alpha_{5\rho}\alpha_6^\rho \sqrt{\frac{\pi\mu R}{2}} K_{1/2}(\mu R) \approx \frac{\alpha^3}{r_{12} r_{34} r_{56} \Delta^2} \alpha_{1\mu}\alpha_2^\mu \alpha_{3\nu}\alpha_4^\nu \alpha_{5\rho}\alpha_6^\rho (\mu R - 1). \tag{46}$$

Thus, it turns out to be a spurious divergence; the IR divergence is ruled out and a finite part remains in the limit $\mu \to 0$. Finally, the IR divergence arising from the third-order pole is treated. The corresponding integral to evaluate is

$$\mathcal{I}_{3,0,0} = \frac{-\alpha^3}{\pi r_{12} r_{34} r_{56}} \alpha_{1\mu}\alpha_2^\mu \alpha_{3\nu}\alpha_4^\nu \alpha_{5\rho}\alpha_6^\rho \sqrt{\frac{\pi R}{2\mu}} \frac{R}{2} K_{1/2}(\mu R) \approx \frac{-\alpha^3 R}{4 r_{12} r_{34} r_{56}} \alpha_{1\mu}\alpha_2^\mu \alpha_{3\nu}\alpha_4^\nu \alpha_{5\rho}\alpha_6^\rho \left(\frac{1}{\mu} - R\right), \tag{47}$$

leading to a singular behavior when the limit $\mu \to 0$ is taken. The behavior of the IR divergence arising from the third-order pole is in agreement with the one presented in Ref. [46], where a similar analysis was performed for the self-energy screening effects in $g$-factor calculations. A different treatment for the regularization of the IR divergence for the third-order pole based on a symmetry argument is proposed in Appendix E. Similarly to the IR divergence arising from the second-order pole, one looks for the compensating crossed diagram to ensure that the total expression is finite.

The explicit cancellation of IR divergences, at the individual Feynman diagram level by the appropriate crossed term, is demonstrated in Table I. An exception is met for the ladder reducible 2 terms, which compensate themselves. A swapping of the indices in the expressions presented in Sec. III might be sometimes necessary in order to make the compensation

TABLE I. IR divergence regularization at the individual Feynman diagram level. IR divergences are found in the reducible expressions, for both ladder and crossed loops. "Crossed" stands for the crossed compensating term. The $\mathcal{I}_{n,m_\pm,p}$ describes the type of divergent integral encountered in the graph. Each term can be found in Sec. III, following the referenced equation. The labels are simplified in comparison to the ones presented there; only the difference between them is highlighted.

| Feynman diagram level | Type of IR divergence | Crossed | IR compensation |
|---|---|---|---|
| | $\Delta E_v^{(3I)3e} \in$ S[V(VP)P]E | | |
| $H_1$: ladder red 1 (23) | $\mathcal{I}_{2,1_+,0}$ | $H_2$: crossed (A1) | $\mathcal{I}_{2,1_-,0}$ |
| $H_1$: ladder red 1(24) | $\mathcal{I}_{2,1_+,0}$ | $H_2$: crossed (A1) | $\mathcal{I}_{2,1_-,0}$ |
| $H_1$: ladder red 2 (25) | $\mathcal{I}_{3,0,0}$ | $H_2$: ladder red 2 (A7) | $\mathcal{I}_{3,0,0}$ |
| $H_1$: crossed red (26) | $\mathcal{I}_{2,1_-,0}$, $\mathcal{I}_{3,0,0}$ | $H_2$: crossed (A1) | $\mathcal{I}_{2,1_-,0}$, $\mathcal{I}_{3,0,0}$ |
| $H_2$: ladder red 1 (A3) | $\mathcal{I}_{2,0,1}$ | $H_1$: crossed irr (21) | $\mathcal{I}_{2,0,1}$ |
| $H_2$: ladder red 1 (A5) | $\mathcal{I}_{2,0,1}$ | $H_1$: crossed irr (20) | $\mathcal{I}_{2,0,1}$ |
| $H_2$: ladder red 2 (A7) | $\mathcal{I}_{3,0,0}$ | $H_1$: ladder red 2 (25) | $\mathcal{I}_{3,0,0}$ |
| | $\Delta E_v^{(3I)3e} \in$ S(VP)EVP | | |
| $F_1$: ladder red 1 (B7) | $\mathcal{I}_{2,0,1}$ | $F_1$: crossed (B3) | $\mathcal{I}_{2,0,1}$ |
| $F_2$: ladder red 1(30) | $\mathcal{I}_{2,1_+,0}$ | $F_2$: crossed (28) | $\mathcal{I}_{2,1_-,0}$ |
| $F_2$: ladder red 1 (31) | $\mathcal{I}_{2,1_+,0}$ | $F_2$: crossed (28) | $\mathcal{I}_{2,1_-,0}$ |
| $F_2$: ladder red 2 (32) | $\mathcal{I}_{3,0,0}$ | $F_2$: crossed (28) | $\mathcal{I}_{3,0,0}$ |
| $F_3$: ladder red 1 (B14) | $\mathcal{I}_{2,0,1}$ | $F_3$: crossed irr (B10) | $\mathcal{I}_{2,0,1}$ |
| $F_3$: ladder red 2 (B15) | $\mathcal{I}_{3,0,0}$ | $F_3$: crossed red (B11) | $\mathcal{I}_{3,0,0}$ |
| $F_3$: crossed red (B11) | $\mathcal{I}_{2,1_-,0}$ | $F_2$: crossed (28) | $\mathcal{I}_{2,1_-,0}$ |

apparent. Moreover, it was shown that IR divergences are absorbed by expressions belonging to the same subset.

## VI. COMPARISON

Two different approaches were utilized to infer a partial third-order interelectronic correction to the energy shift. A comparison between the results of each of these two approaches is undertaken in this section.

The discussion begins with the four-electron contribution, which involves three types of terms: the irreducible [$\Delta E_v^{(3I)4e,irr}$ (D1) and (D2)], the reducible 1 [$\Delta E_v^{(3I)4e,red1}$ (D3) and (D4)], and the reducible 2 [$\Delta E_v^{(3I)4e,red2}$ (D5) and (D6)]. For every type previously stated, agreement between the perturbative treatment of the $\mathcal{V}$-perturbed S(VP)E three-electron subset and the effective one-particle approach is met.

For the three-electron contribution, an identical separation to the above is conducted. The irreducible type is composed of three parts, two of which correspond to crossed diagrams [$\Delta E_v^{(3I)3e,cross}$ (C4) and (C5) and $\Delta E_v^{(3I)3e,cross,irr}$ (C2) and (C3)] and one corresponding to ladder diagrams [$\Delta E_v^{(3I)3e,lad,irr}$ (C6) and (C7)]. The outcomes of the two methods are in full concordance for these terms. Regarding the reducible 1 type, the cross reducible [$\Delta E_v^{(3I)3e,cross,red}$ (C8) and (C9)] and the ladder reducible 1 IR free $\omega$ [$\Delta E_{v,\text{IR free }\omega}^{(3I)lad,red1}$ (C14) and (C15)] terms extracted from the two treatments are in good agreement.

However, for the remaining reducible 1 terms [$\Delta E_{v,\text{IR div}}^{(3I)3e,lad,red1}$ (C10) and (C11) and $\Delta E_{v,\text{IR free}}^{(3I)3e,lad,red1}$ (C12) and (C13)] a discrepancy is encountered. Yerokhin *et al.*, in Ref. [45], already pointed out that the perturbation theory approach runs into trouble dealing with reducible terms.[4] They invoked gauge invariance to fix the problem. If proceeding as explained at the beginning of the section dedicated to perturbation theory approach, a problem identical to the one highlighted by Yerokhin *et al.* is met, namely, that the poles differ by the sign of the $i\varepsilon$ prescription,

$$\frac{1}{(\omega+i\varepsilon)(-\omega+i\varepsilon)} \quad \text{vs} \quad \frac{1}{(\omega+i\varepsilon)^2} \text{ or } \frac{1}{(-\omega+i\varepsilon)^2}, \tag{48}$$

when facing ladder reducible 1 terms $\Delta E_{v,\text{IR div}}^{(3I)3e,lad,red1}$ and $\Delta E_{v,\text{IR free}}^{(3I)3e,lad,red1}$. The difference in the topology of the poles arises from unaccounted restrictions in the summations. Surprisingly, and possibly related to the topology problem associated with the poles, the two approaches differ regarding the extra terms

$$\Delta E_{v,\text{S[V(VP)P]E}}^{(3I)3e,red1} = \sum_{a,b,b_1,v_1,i}^{i\neq v} \frac{I_{vbb_1v_1}(\Delta_{vb})I_{v_1aia}(0)I_{ib_1bv}(\Delta_{vb})}{(\epsilon_v-\epsilon_i)^2} \tag{49}$$

and

$$\Delta E_{v,\text{S(VP)EVP}}^{(3I)3e,red1} = -\sum_{a,b,b_1,v_1,i}^{i\neq b} \frac{I_{vbb_1v_1}(\Delta_{vb})I_{b_1aia}(0)I_{iv_1vb}(\Delta_{vb})}{(\epsilon_b-\epsilon_i)^2}. \tag{50}$$

These are not found via the perturbative analysis but are present in the redefined vacuum state approach. They are obtained as the interplay among terms generated from the ladder reducible 1 terms, upon the symmetrization of the energy flow in the loop, and four-electron reducible 1 terms. The former originates from $H_1$ while the latter originate from $F_2$. They look like the four-electron reducible 1 contribution, due to the absence of the $\omega$ integration. According to the gauge invariance of the three-electron S(VP)E subset of the two-photon-exchange corrections, they should be incorporated in the three-electron contribution of the three-photon-exchange corrections. The structure of these terms suggests that they are included in the reducible 1 contribution. The last point to

[4]See remarks below Eqs. (32), (35), and (37) in Ref. [45].

be made concerning these two terms is that they are obviously IR finite.

The reducible 2 type contains only ladder reducible 2 terms: the IR free one [$\Delta E_{v,\text{IR free}}^{(3I)3e,lad,red2}$ (C18) and (C19)] and the IR divergent one [$\Delta E_{v,\text{IR div}}^{(3I)3e,lad,red2}$ (C16) and (C17)]. The expressions obtained from the two different methods are identical.

Overall, if errors occurred in the different three-electron types of interelectronic interactions considered, one would expect to see repercussions in the four-electron contribution. In this case, the four-electron contribution would suffer from discrepancies between the two methods, a behavior which is not encountered. Therefore, these two independent derivations and the comparison of the resulting expressions presented in the present work are fully consistent, except for two expressions mentioned above. In these cases, the discrepancy can be traced back to unaccounted for restrictions in the summations, resulting in a different topology of the poles. Furthermore, the derivation based on this two-method scheme is a good sanity check of the obtained formulas. The perturbation theory approach also helps to sort out the three- and four-electron contributions, especially for the extra terms given in Eqs. (49) and (50). In summary, the gathered evidence points towards the consistency of the derived three-electron expressions. Moreover, the excellent agreement met at the four-electron contribution level serves as a strong indication that the three-electron expressions should be reliable.

Concerning the separation into the proposed GI subsets S[V(VP)P]E and S(VP)EVP, the cancellation of IR divergences by elements from the same subset is very assuring. A numerical evaluation of the derived expressions is the sole way to either invalidate the conjectured separability into the GI subsets put forward here, based on analytical considerations, or confirm it and therewith turn it into a solid claim.

## VII. DISCUSSION AND CONCLUSION

The expressions presented in the work can readily be applied to any Li-like and/or B-like atoms or ions. They represent an important step towards the evaluation of third-order interelectronic interactions. The three-photon-exchange formulas were explicitly derived for two proposed GI subsets arising from two classes of one-particle three-loop Feynman diagrams. The derivation relies on an effective one-particle approach, owing to the redefinition of the vacuum state, in the framework of the TTGF method. The resulting formulas contained infrared divergences. They were investigated and regularized by the introduction of a photon mass term. Two different types of divergences were encountered when the photon mass was sent to zero: a logarithmic one (43) and a first-order singular one (47). The divergent behaviors observed are in full accordance with previous studies [23,46]. In order to allow for a verification of the expressions derived in the framework of the TTGF method, an independent derivation was conducted with the help of perturbation theory. However, from the very beginning of the study, the issue of the topology of the pole was known for the second method (see the detailed explanation in the work of Yerokhin *et al.* [45]). Nevertheless, the idea of the present work was to see how far one can get with the cross-check, relying on the possibility of a perturbative treatment. This helped to resolve the different reducible terms (red1 and red2) and to sort out the distribution of different (three-electron and four-electron) contributions in each expression of the subsets (S[V(VP)P]E and S(VP)EVP). The agreement between the two approaches, at the four-electron level, is excellent. At the three-electron level, reasonable agreement is met between the two results. Here the discrepancy related to the different topology of the poles encountered in the (three-electron) ladder reducible 1 terms, for both IR divergent and IR finite ones, prevents complete agreement. The difference in the topology of the poles could be attributed to unaccounted for restrictions in summations. In fact, such a discrepancy in the topology of the poles was already encountered when comparing the results for the two-photon-exchange contributions between Refs. [21,56] and Ref. [24].[5] The comparison between the results for the two-photon-exchange two-electron contributions showed that the difference in the topology of the poles did not affect significantly the numerical values; the difference amounts to $O(7 \times 10^{-4})$ atomic unit, or $O(1.9 \times 10^{-2})$ eV. An open question is whether the extra terms are related to this issue and if the role they are playing potentially is to ensure gauge invariance.

Based on the intuition acquired within the perturbative treatment, we do believe that the strong constraint of gauge invariance can be tracked to the third order as well. Hence, it should be expected that the results derived from this approach also fulfill the requirement of gauge invariance. Thus, in analogy to the perturbation theory approach, our belief is that the outcome of the TTGF method is also characterized by the important paradigm of gauge invariance. Whether a further separation according to the subsets is possible cannot be resolved yet. Nevertheless, from the TTGF perspective, the explicit cancellation of IR divergences, within each subset, is very engaging. Finally, a successful verification of the derived expressions was also carried out for the three-electron contribution with the $g$-factor formulas derived in Ref. [29], under the replacement (37). Note that the extra terms are also present in those formulas; they manifest when one proceeds to numerical evaluations [57].

To conclude, the method based on a vacuum state redefinition in QED has been shown, in this work, to be a well-suited tool to perform elaborate calculations. In contrast to other methods, it permits the identification of GI subsets and thus inherently validates the consistency of the obtained results. This asset can be very useful in future derivations of higher-order contributions since it provides a robust verification. Building on this intrinsic characteristic and to highlight the possibility of applying the formalism for advanced calculations, an investigation of third-order interelectronic corrections was carried out. Moreover, the identification of GI expressions

[5]The same problem was met when comparing the two-photon-exchange expressions with the ones derived by Sapirstein and Cheng [see below Eq. (79) in [24]].

within this approach paves the way for calculating higher-order corrections, which can be split into GI subsets and tackled one after the other. The presented redefined vacuum state approach can be further employed for atoms with a (more) sophisticated electronic structure, as it allows one to focus only on the particles that differentiate between the configurations.


## ACKNOWLEDGMENTS

This work was supported by Bundesministerium für Bildung und Forschung through Project No. 05P21SJFAA. R.N.S. is grateful to A. V. Volotka for helpful discussions and to F. Karbstein for helpful comments.


## APPENDIX A: THREE-ELECTRON TERMS ARISING FROM THE $H_2$ DIAGRAM

The expressions extracted from the $H_2$ Feynman diagram are found as follows:

$$\Delta E^{(3\mathrm{I})3\mathrm{e,cross}}_{v,H_2} = \frac{i}{2\pi}\int d\omega \sum_{i,j,k} \frac{I_{vjib}(\omega) I_{kaja}(0) I_{bikv}(\omega)}{(\epsilon_v-\omega-\epsilon_i u)(\epsilon_b-\omega-\epsilon_j u)(\epsilon_b-\omega-\epsilon_k u)}, \tag{A1}$$

$$\Delta E^{(3\mathrm{I})3\mathrm{e,lad,irr}}_{v,H_2} = \frac{i}{2\pi}\int d\omega \sum_{i,j,k}^{k\neq b,\{i,j\}\neq\{b,v\}} \frac{I_{vbij}(\omega) I_{kaba}(0) I_{jikv}(\omega)}{(\epsilon_v-\omega-\epsilon_i u)(\epsilon_b+\omega-\epsilon_j u)(\epsilon_b-\epsilon_k u)}, \tag{A2}$$

$$\Delta E^{(3\mathrm{I})3\mathrm{e,lad,red1}}_{v,H_2} = -\frac{i}{2\pi}\int d\omega \sum_{i,j,k}^{k\neq b,\{i,j\}=\{b,v\}} \frac{I_{vbij}(\omega) I_{kaba}(0) I_{jikv}(\omega)}{(\epsilon_v-\omega-\epsilon_i u)^2(\epsilon_b-\epsilon_k u)}, \tag{A3}$$

$$\Delta E^{(3\mathrm{I})3\mathrm{e,lad,irr}}_{v,H_2} = \frac{i}{2\pi}\int d\omega \sum_{i,j,k}^{k\neq b,\{i,j\}\neq\{b,v\}} \frac{I_{vkij}(\omega) I_{baka}(0) I_{jibv}(\omega)}{(\epsilon_v-\omega-\epsilon_i u)(\epsilon_b+\omega-\epsilon_j u)(\epsilon_b-\epsilon_k u)}, \tag{A4}$$

$$\Delta E^{(3\mathrm{I})\mathrm{lad,red1}}_{v,H_2} = -\frac{i}{2\pi}\int d\omega \sum_{i,j,k}^{k\neq b,\{i,j\}=\{b,v\}} \frac{I_{vkij}(\omega) I_{baka}(0) I_{jibv}(\omega)}{(\epsilon_v-\omega-\epsilon_i u)^2(\epsilon_b-\epsilon_k u)}. \tag{A5}$$

The nondiagrammatic term for $H_2$ are found to be

$$\Delta E^{(3\mathrm{I})3\mathrm{e,lad,red1}}_{v,H_2} = -\frac{i}{2\pi}\int d\omega \sum_{i,j}^{\{i,j\}\neq\{b,v\}} \frac{I_{vbij}(\omega) I_{b_1aba}(0) I_{jib_1v}(\omega)}{(\epsilon_v-\omega-\epsilon_i u)(\epsilon_b+\omega-\epsilon_j u)^2}, \tag{A6}$$

$$\Delta E^{(3\mathrm{I})3\mathrm{e,lad,red2}}_{v,H_2} = -\frac{i}{2\pi}\int d\omega \sum_{i,j}^{\{i,j\}=\{b,v\}} \frac{I_{vbij}(\omega) I_{b_1aba}(0) I_{jib_1v}(\omega)}{(\epsilon_v-\omega-\epsilon_i u)^3}. \tag{A7}$$

## APPENDIX B: THREE-ELECTRON TERMS ARISING FROM THE $F_1$ AND $F_3$ DIAGRAMS

Within this subset, the Green's function associated with the remaining diagrams reads

$$\Delta g^{(3)F_1}_{\alpha,vv}(E) = \frac{1}{(E-\epsilon_v)^2}\left(\frac{i}{2\pi}\right)^3 \sum_{i,j,k,l,p}\int d\omega dk_1 dk_2 \frac{I_{viji}(0)}{\big[k_1-\epsilon_i+i\varepsilon\big(\epsilon_i-E^F_\alpha\big)\big]\big[E-\epsilon_j+i\varepsilon\big(\epsilon_j-E^F_\alpha\big)\big]} \times \frac{I_{jpkl}(\omega) I_{klvp}(\omega)}{\big[E-\omega-\epsilon_k+i\varepsilon\big(\epsilon_k-E^F_\alpha\big)\big]\big[k_2-\epsilon_l+i\varepsilon\big(\epsilon_l-E^F_\alpha\big)\big]\big[k_2-\omega-\epsilon_p+i\varepsilon\big(\epsilon_p-E^F_\alpha\big)\big]} \tag{B1}$$

for $F_1$ and

$$\Delta g^{(3)F_3}_{\alpha,vv}(E) = \frac{1}{(E-\epsilon_v)^2}\left(\frac{i}{2\pi}\right)^3 \sum_{i,j,k,l,p}\int d\omega dk_1 dk_2 \frac{I_{vkij}(\omega)}{\big[E-\omega-\epsilon_i+i\varepsilon\big(\epsilon_i-E^F_\alpha\big)\big]\big[k_1-\epsilon_j+i\varepsilon\big(\epsilon_j-E^F_\alpha\big)\big]} \times \frac{I_{ijlk}(\omega) I_{lpvp}(0)}{\big[k_1-\omega-\epsilon_k+i\varepsilon\big(\epsilon_k-E^F_\alpha\big)\big]\big[E-\epsilon_l+i\varepsilon\big(\epsilon_l-E^F_\alpha\big)\big]\big[k_2-\epsilon_p+i\varepsilon\big(\epsilon_p-E^F_\alpha\big)\big]} \tag{B2}$$

for $F_3$. The extraction procedure is carried out for the $F_1$ Feynman diagram, which contributes as follows. The terms associated with the crossed graphs are

$$\Delta E^{(3\mathrm{I})3\mathrm{e,cross,irr}}_{v,F_1} = \frac{i}{2\pi}\int d\omega \sum_{i,j,k}^{i\neq v} \frac{I_{vaia}(0) I_{ikjb}(\omega) I_{bjkv}(\omega)}{(\epsilon_v-\epsilon_i)(\epsilon_v-\omega-\epsilon_j u)(\epsilon_b-\omega-\epsilon_k u)}, \tag{B3}$$

$$\Delta E^{(3I)3e,cross,red1}_{v,F_1} = -\frac{i}{2\pi}\int d\omega \sum_{i,j} \frac{I_{vav_1a}(0) I_{v_1kjb}(\omega) I_{bjkv}(\omega)}{(\epsilon_v - \omega - \epsilon_j u)^2(\epsilon_b - \omega - \epsilon_k u)}. \tag{B4}$$

The expressions corresponding to the ladder-loop graph read

$$\Delta E^{(3I)3e,lad,irr}_{v,F_1} = \frac{i}{2\pi}\int d\omega \sum_{i,j,k}^{i\neq v,\{j,k\}\neq\{v,b\}} \frac{I_{vaia}(0) I_{ibjk}(\omega) I_{jkvb}(\omega)}{(\epsilon_v - \epsilon_i u)(\epsilon_v - \omega - \epsilon_j u)(\epsilon_b + \omega - \epsilon_k u)}, \tag{B5}$$

$$\Delta E^{(3I)3e,lad,red1}_{v,F_1} = -\frac{i}{2\pi}\int d\omega \sum_{i,j,k}^{\{j,k\}\neq\{v,b\}} \frac{I_{vav_1a}(0) I_{v_1bjk}(\omega) I_{jkvb}(\omega)}{(\epsilon_v - \omega - \epsilon_j u)^2(\epsilon_b + \omega - \epsilon_k u)}, \tag{B6}$$

$$\Delta E^{(3I)3e,lad,red1}_{v,F_1} = -\frac{i}{2\pi}\int d\omega \sum_{i,j,k}^{i\neq v,\{j,k\}=\{v,b\}} \left[\frac{I_{vaia}(0) I_{ibjk}(\omega) I_{jkvb}(\omega)}{(\epsilon_v - \epsilon_i u)^2}\left(\frac{1}{(\epsilon_v - \omega - \epsilon_j u)} + \frac{1}{(\epsilon_b + \omega - \epsilon_k u)}\right)\right.$$
$$\left. + \frac{I_{vaia}(0) I_{ibjk}(\omega) I_{jkvb}(\omega)}{(\epsilon_v - \epsilon_i u)(\epsilon_v - \omega - \epsilon_j u)^2}\right], \tag{B7}$$

$$\Delta E^{(3I)3e,lad,red2}_{v,F_1} = \frac{i}{2\pi}\int d\omega \sum_{j,k}^{\{j,k\}=\{v,b\}} \frac{I_{vav_1a}(0) I_{v_1bjk}(\omega) I_{jkvb}(\omega)}{(\epsilon_v - \omega - \epsilon_j u)^3}. \tag{B8}$$

For the disconnected parts, the terms presented below cancel the reducible elements found in $F_1$, namely, the term in the first line cancels (B4), the term in the second line cancels (B6), and the term in the third line cancels (B8). It leaves only the irreducible expressions and the ladder reducible 1 term (B7):

$$\Delta E^{(3I)3e,disc}_{v,F} = \frac{i}{2\pi}\int d\omega \left(\sum_{i,j} \frac{I_{vava}(0) I_{v_1jib}(\omega) I_{ibv_1j}(\omega)}{(\epsilon_v - \omega - \epsilon_i u)^2(\epsilon_b - \omega - \epsilon_j u)} + \sum_{i,j}^{\{i,j\}\neq\{b,v\}} \frac{I_{vava}(0) I_{v_1bij}(\omega) I_{ijv_1bj}(\omega)}{(\epsilon_v - \omega - \epsilon_i u)^2(\epsilon_b + \omega - \epsilon_j u)}\right.$$
$$\left. - \sum_{i,j}^{\{i,j\}=\{b,v\}} \frac{I_{vava}(0) I_{v_1bij}(\omega) I_{ijv_1bj}(\omega)}{(\epsilon_v - \omega - \epsilon_i u)^3}\right). \tag{B9}$$

From the $F_3$ Feynman diagram, the following terms arise. Similarly to the $F_1$ graph, the terms corresponding to the crossed graph are

$$\Delta E^{(3I)3e,cross,irr}_{v,F_3} = \frac{i}{2\pi}\int d\omega \sum_{i,j,k}^{k\neq v} \frac{I_{vjib}(\omega) I_{ibkj}(\omega) I_{kava}(0)}{(\epsilon_v - \omega - \epsilon_i u)(\epsilon_b - \omega - \epsilon_j u)(\epsilon_v - \epsilon_k u)}, \tag{B10}$$

$$\Delta E^{(3I)3e,cross,red}_{v,F_3} = \frac{-i}{2\pi}\int d\omega \sum_{i,j} \frac{I_{vjib}(\omega) I_{ibv_1j}(\omega) I_{v_1ava}(0)}{(\epsilon_v - \omega - \epsilon_i u)^2(\epsilon_b - \omega - \epsilon_j u)}. \tag{B11}$$

The ones associated with the ladder graph read

$$\Delta E^{(3I)3e,lad,irr}_{v,F_3} = \frac{i}{2\pi}\int d\omega \sum_{i,j,k}^{\{i,j\}\neq\{b,v\},k\neq v} \frac{I_{vbij}(\omega) I_{ijkb}(\omega) I_{kava}(0)}{(\epsilon_v - \omega - \epsilon_i u)(\epsilon_b + \omega - \epsilon_j u)(\epsilon_v - \epsilon_k u)}, \tag{B12}$$

$$\Delta E^{(3I)lad,red1}_{v,F_3} = \frac{-i}{2\pi}\int d\omega \sum_{i,j}^{\{i,j\}\neq\{b,v\}} \frac{I_{vbij}(\omega) I_{ijv_1b}(\omega) I_{v_1ava}(0)}{(\epsilon_v - \omega - \epsilon_i u)^2(\epsilon_b + \omega - \epsilon_j u)}, \tag{B13}$$

$$\Delta E^{(3I)3e,lad,red1}_{v,F_3} = \frac{-i}{2\pi}\int d\omega \sum_{i,j,k}^{\{i,j\}=\{b,v\},k\neq v} \left[\frac{I_{vbij}(\omega) I_{ijkb}(\omega) I_{kava}(0)}{(\epsilon_v - \epsilon_k u)^2}\left(\frac{1}{(\epsilon_v - \omega - \epsilon_i u)} + \frac{1}{(\epsilon_b + \omega - \epsilon_j u)}\right)\right.$$
$$\left. + \frac{I_{vbij}(\omega) I_{ijkb}(\omega) I_{kava}(0)}{(\epsilon_v - \omega - \epsilon_i u)^2(\epsilon_v - \epsilon_k u)}\right], \tag{B14}$$

$$\Delta E^{(3I)3e,lad,red2}_{v,F_3} = \frac{i}{2\pi}\int d\omega \sum_{i,j}^{\{i,j\}=\{b,v\}} \frac{I_{vbij}(\omega) I_{ijv_1b}(\omega) I_{v_1ava}(0)}{(\epsilon_v - \omega - \epsilon_i u)^3}. \tag{B15}$$

## APPENDIX C: THIRD-ORDER INTERELECTRONIC CORRECTIONS DERIVED BY A PERTURBATIVE TREATMENT: THE THREE-ELECTRON SUBSET

The idea is to proceed as follows: One perturbs the S(VP)E two-electron expressions (12) and (13) according to Eqs. (33)–(36) and finds the desired formulas under the replacement (37). However, the issue is, as already pointed out by Yerokhin *et al.* in Ref. [45], that this approach suffers from troubles dealing with reducible terms (see footnote 4). They invoked gauge invariance to fix the problem. If proceeding as explained just above, a problem identical to the one highlighted by Yerokhin *et al.* is met, namely, that the poles differ by the sign of the $i\varepsilon$ prescription (see footnote 5),

$$\frac{1}{(\omega+i\varepsilon)(-\omega+i\varepsilon)} \quad \text{vs} \quad \frac{1}{(\omega+i\varepsilon)^2} \text{ or } \frac{1}{(-\omega+i\varepsilon)^2}, \tag{C1}$$

when facing ladder reducible 1 contributions $\Delta E^{(3I)3e,lad,red1}_{v,\text{IR div}}$ and $\Delta E^{(3I)3e,lad,red1}_{v,\text{IR free}}$. The difference in the topology of the poles arises from unaccounted restrictions in the summations. Nevertheless, for the sake of the verification, it is worth tackling this perturbative analysis to see how far one can get. However, due to this previous discrepancy, the different three-electron terms presented below are those derived within the redefinition of the vacuum state formalism. They are separated into irreducible (irr), reducible 1 (red1), and reducible 2 (red2) types and moreover into S[V(VP)P]E and S(VP)EVP according to their origin diagrams.

### 1. Irreducible terms

The crossed irreducible expression, a new feature showing up at this order, is presented first. A separation related to each subset is conducted,

$$\Delta E^{(3I)3e,cross,irr}_{v,S[V(VP)P]E} = \frac{i}{2\pi}\int d\omega \sum_{a,b,i,j,k}^{k\neq b} \frac{I_{vjib}(\omega)I_{baka}(0)I_{ikvj}(\omega) + I_{vjik}(\omega)I_{kaba}(0)I_{ibvj}(\omega)}{(\epsilon_v-\omega-\epsilon_i u)(\epsilon_b-\omega-\epsilon_j u)\Delta_{bk}}, \tag{C2}$$

$$\Delta E^{(3I)3e,cross,irr}_{v,S(VP)EVP} = \frac{i}{2\pi}\int d\omega \sum_{a,b,i,j,k}^{i\neq v} \frac{I_{vaia}(0)I_{ikjb}(\omega)I_{bjkv}(\omega) + I_{vkjb}(\omega)I_{jbik}(\omega)I_{aiav}(0)}{\Delta_{vi}(\epsilon_v-\omega-\epsilon_j u)(\epsilon_b-\omega-\epsilon_k u)}. \tag{C3}$$

Then the crossed expression, also separated according to its origin diagram, is displayed,

$$\Delta E^{(3I)3e,cross}_{v,S[V(VP)P]E} = \frac{i}{2\pi}\int d\omega \sum_{a,b,i,j,k} \frac{I_{vjib}(\omega)I_{akaj}(0)I_{ibvk}(\omega)}{(\epsilon_v-\omega-\epsilon_i u)(\epsilon_b-\omega-\epsilon_j u)(\epsilon_b-\omega-\epsilon_k u)}, \tag{C4}$$

$$\Delta E^{(3I)3e,cross}_{v,S(VP)EVP} = \frac{i}{2\pi}\int d\omega \sum_{a,b,i,j,k} \frac{I_{vkib}(\omega)I_{iaja}(0)I_{bjkv}(\omega)}{(\epsilon_v-\omega-\epsilon_i u)(\epsilon_v-\omega-\epsilon_j u)(\epsilon_b-\omega-\epsilon_k u)}. \tag{C5}$$

Finally, the ladder irreducible expression is found as

$$\begin{aligned}\Delta E^{(3I)3e,lad,irr}_{v,S[V(VP)P]E} = \frac{i}{2\pi}\int d\omega \Bigg( &\sum_{a,b,i,j,k}^{k\neq b,\{i,j\}\neq\{v,b\}} \frac{I_{vbij}(\omega)I_{akab}(0)I_{ijvk}(\omega) + I_{vkij}(\omega)I_{abak}(0)I_{ijvb}(\omega)}{(\epsilon_v-\omega-\epsilon_i u)(\epsilon_b+\omega-\epsilon_j u)\Delta_{bk}} \\ &+ \sum_{a,b,i,j,k}^{\{i,j\}\neq\{v,b\},\{i,k\}\neq\{v,b\}} \frac{I_{vbij}(\omega)I_{jaka}(0)I_{ikvb}(\omega)}{(\epsilon_v-\omega-\epsilon_i u)(\epsilon_b+\omega-\epsilon_j u)(\epsilon_b+\omega-\epsilon_k u)}\Bigg),\end{aligned} \tag{C6}$$

$$\begin{aligned}\Delta E^{(3I)3e,lad,irr}_{v,S(VP)EVP} = \frac{i}{2\pi}\int d\omega \Bigg( &\sum_{a,b,i,j,k}^{i\neq v,\{j,k\}\neq\{v,b\}} \frac{I_{vaia}(0)I_{ibjk}(\omega)I_{kjbv}(\omega) + I_{vbjk}(\omega)I_{jkib}(\omega)I_{aiav}(0)}{\Delta_{vi}(\epsilon_v-\omega-\epsilon_j u)(\epsilon_b+\omega-\epsilon_k u)} \\ &+ \sum_{a,b,i,j,k}^{\{i,k\}\neq\{v,b\},\{j,k\}\neq\{v,b\}} \frac{I_{vbik}(\omega)I_{iaja}(0)I_{kjbv}(\omega)}{(\epsilon_v-\omega-\epsilon_i u)(\epsilon_v-\omega-\epsilon_j u)(\epsilon_b+\omega-\epsilon_k u)}\Bigg).\end{aligned} \tag{C7}$$

### 2. Reducible 1 terms

Since a crossed irreducible expression exists, the associated crossed reducible terms are found and worked out. The result is separated as well according to the originating subset and reads

$$\Delta E^{(3\mathrm{I})3\mathrm{e},\mathrm{cross},\mathrm{red}}_{v,\mathrm{S[V(VP)P]E}} = -\frac{i}{2\pi}\int d\omega \sum_{a,b,b_1,i,j} \frac{I_{vjib}(\omega) I_{bab_1a}(0) I_{ib_1vj}(\omega)}{(\epsilon_v-\omega-\epsilon_i u)(\epsilon_b-\omega-\epsilon_j u)^2}, \tag{C8}$$

$$\Delta E^{(3\mathrm{I})3\mathrm{e},\mathrm{cross},\mathrm{red}}_{v,\mathrm{S(VP)EVP}} = -\frac{i}{2\pi}\int d\omega \sum_{a,b,v_1,i,j} \frac{I_{vjib}(\omega) I_{bijv_1}(\omega) I_{av_1av}(0)}{(\epsilon_v-\omega-\epsilon_i u)^2(\epsilon_b-\omega-\epsilon_j u)}. \tag{C9}$$

Each ladder reducible 1 term is separated into an IR free and an IR divergent part and displayed according to its provenance. Beginning with the latter, one has

$$\begin{aligned}\Delta E^{(3\mathrm{I})3\mathrm{e},\mathrm{lad},\mathrm{red1}}_{v,\mathrm{S[V(VP)P]E,IR\ div}} = -\frac{i}{2\pi}\int \frac{d\omega}{(-\omega+i\varepsilon)^2} \sum_{a,b,b_1,v_1,i}^{i\neq b} \Bigg( & \frac{I_{vbv_1b_1}(\omega) I_{aiab}(0) I_{v_1b_1vi}(\omega) + I_{viv_1b_1}(\omega) I_{abai}(0) I_{v_1b_1vb}(\omega)}{\Delta_{bi}} \\ & + \frac{I_{vbv_1b_1}(\omega) I_{b_1aia}(0) I_{v_1ivb}(\omega) + I_{vbv_1i}(\omega) I_{iab_1a}(0) I_{v_1b_1vb}(\omega)}{(\Delta_{bi}+\omega+i\varepsilon)} \Bigg),\end{aligned} \tag{C10}$$

$$\begin{aligned}\Delta E^{(3\mathrm{I})3\mathrm{e},\mathrm{lad},\mathrm{red1}}_{v,\mathrm{S(VP)EVP,IR\ div}} = -\frac{i}{2\pi}\int \frac{d\omega}{(-\omega+i\varepsilon)^2} \sum_{a,b,b_1,v_1,i}^{i\neq v} \Bigg( & \frac{I_{vaia}(0) I_{ibv_1b_1}(\omega) I_{b_1v_1bv}(\omega) + I_{vbv_1b_1}(\omega) I_{v_1b_1ib}(\omega) I_{aiav}(0)}{\Delta_{vi}} \\ & + \frac{I_{vbib_1}(\omega) I_{iav_1a}(0) I_{b_1v_1bv}(\omega) + I_{vbv_1b_1}(\omega) I_{v_1aia}(0) I_{b_1ibv}(\omega)}{(\Delta_{vi}-\omega+i\varepsilon)} \Bigg)\end{aligned} \tag{C11}$$

for the IR divergent part. The IR finite part is further separated, because its first part is the counterpart of the previously introduced IR divergent terms,

$$\begin{aligned}\Delta E^{(3\mathrm{I})3\mathrm{e},\mathrm{lad},\mathrm{red1}}_{v,\mathrm{S[V(VP)P]E,IR\ free}} = & -\frac{i}{4\pi}\int d\omega \Bigg( \frac{1}{(\Delta_{vb}-\omega+i\varepsilon)^2} + \frac{1}{(\Delta_{vb}-\omega-i\varepsilon)^2} \Bigg) \\ & \times \Bigg( \sum_{a,b,b_1,v_1,i}^{i\neq v} \frac{I_{vbb_1v_1}(\omega) I_{v_1aia}(0) I_{b_1ivb}(\omega) + I_{vbb_1i}(\omega) I_{iav_1a}(0) I_{b_1v_1vb}(\omega)}{(\Delta_{bi}+\omega+i\varepsilon)} \\ & + \sum_{a,b,b_1,v_1,i}^{i\neq b} \frac{I_{vbb_1v_1}(\omega) I_{aiab}(0) I_{b_1v_1vi}(\omega) + I_{vib_1v_1}(\omega) I_{abai}(0) I_{b_1v_1vb}(\omega)}{\Delta_{bi}} \Bigg),\end{aligned} \tag{C12}$$

$$\begin{aligned}\Delta E^{(3\mathrm{I})3\mathrm{e},\mathrm{lad},\mathrm{red1}}_{v,\mathrm{S(VP)EVP,IR\ free}} = & -\frac{i}{4\pi}\int d\omega \Bigg( \frac{1}{(\Delta_{vb}-\omega+i\varepsilon)^2} + \frac{1}{(\Delta_{vb}-\omega-i\varepsilon)^2} \Bigg) \\ & \times \Bigg( \sum_{a,b,b_1,v_1,i}^{i\neq v} \frac{I_{vaia}(0) I_{ibb_1v_1}(\omega) I_{v_1b_1bv}(\omega) + I_{vbb_1v_1}(\omega) I_{b_1v_1ib}(\omega) I_{aiav}(0)}{\Delta_{vi}} \\ & + \sum_{a,b,b_1,v_1,i}^{i\neq b} \frac{I_{vbb_1v}(\omega) I_{b_1aia}(0) I_{v_1ibv}(\omega) + I_{vbiv_1}(\omega) I_{iab_1a}(0) I_{v_1b_1bv}(\omega)}{(\Delta_{vi}-\omega+i\varepsilon)} \Bigg),\end{aligned} \tag{C13}$$

while its second part is simply the terms excluded in sums of certain diagrams,

$$\Delta E^{(3\mathrm{I})3\mathrm{e},\mathrm{lad},\mathrm{red1}}_{v,\mathrm{S[V(VP)P]E,IR\ free}\ \omega} = -\frac{i}{2\pi}\int d\omega \sum_{a,b,b_1,i,j}^{\{i,j\}\neq\{v,b\}} \frac{I_{vbij}(\omega) I_{ab_1ab}(0) I_{ijvb_1}(\omega)}{(\epsilon_v-\omega-\epsilon_i u)(\epsilon_b+\omega-\epsilon_j u)^2}, \tag{C14}$$

$$\Delta E^{(3\mathrm{I})3\mathrm{e},\mathrm{lad},\mathrm{red1}}_{v,\mathrm{S(VP)EVP,IR\ free}\ \omega} = -\frac{i}{2\pi}\int d\omega \sum_{a,b,v_1,i,j}^{\{i,j\}\neq\{v,b\}} \frac{I_{vbij}(\omega) I_{ijv_1b}(\omega) I_{av_1av}(0)}{(\epsilon_v-\omega-\epsilon_i u)^2(\epsilon_b+\omega-\epsilon_j u)}. \tag{C15}$$

### 3. Reducible 2 terms

Facing now the reducible 2 contribution, the identical separation into IR divergent and IR free terms is conducted, in addition to the distinction between the two different subsets. The IR divergent terms are

$$\Delta E^{(3\mathrm{I})3\mathrm{e,lad,red2}}_{v,\mathrm{S[V(VP)P]E,IR\ div}} = \frac{i}{2\pi}\int \frac{d\omega}{(-\omega+i\varepsilon)^3} \sum_{a,b,b_1,b_2,v_1} \big[I_{vbv_1b_1}(\omega) I_{b_1ab_2a}(0) I_{v_1b_2vb}(\omega) - I_{vbv_1b_2}(\omega) I_{ab_1ab}(0) I_{v_1b_2vb_1}(\omega)\big], \tag{C16}$$

$$\Delta E^{(3\mathrm{I})3\mathrm{e,lad,red2}}_{v,\mathrm{S(VP)EVP,IR\ div}} = \frac{i}{2\pi}\int \frac{d\omega}{(-\omega+i\varepsilon)^3} \sum_{a,b,b_1,v_1,v_2} \big[I_{vbv_1b_1}(\omega) I_{v_1b_1v_2b}(\omega) I_{av_2av}(0) - I_{vbv_1b_1}(\omega) I_{v_1av_2a}(0) I_{b_1v_2bv}(\omega)\big] \tag{C17}$$

and the IR free ones are

$$\Delta E^{(3\mathrm{I})3\mathrm{e,lad,red2}}_{v,\mathrm{S[V(VP)P]E,IR\ free}} = \frac{i}{4\pi}\int d\omega \left(\frac{1}{(\Delta_{vb}-\omega+i\varepsilon)^3} + \frac{1}{(\Delta_{vb}-\omega-i\varepsilon)^3}\right) \times \left(\sum_{a,b,b_1,v_1,v_2} I_{vbb_1v_1}(\omega) I_{v_1av_2a}(0) I_{b_1v_2vb}(\omega) - \sum_{a,b,b_1,,b_2,v_1} I_{vbb_2v_1}(\omega) I_{ab_1ab}(0) I_{b_2v_1vb_1}(\omega)\right), \tag{C18}$$

$$\Delta E^{(3\mathrm{I})3\mathrm{e,lad,red2}}_{v,\mathrm{S(VP)EVP,IR\ free}} = \frac{i}{4\pi}\int d\omega \left(\frac{1}{(\Delta_{vb}-\omega+i\varepsilon)^3} + \frac{1}{(\Delta_{vb}-\omega-i\varepsilon)^3}\right)\left(\sum_{a,b,b_1,v_1,v_2} I_{vbb_1v_1}(\omega) I_{b_1v_1v_2b}(\omega) I_{av_2av}(0) - \sum_{a,b,b_1,b_2,v_1} I_{vbb_1v_1}(\omega) I_{b_2v_1vb}(\omega) I_{b_1ab_2a}(0)\right). \tag{C19}$$

### 4. Extra terms

The remaining terms

$$\Delta E^{(3\mathrm{I})3\mathrm{e,red1}}_{v,\mathrm{S[V(VP)P]E}} = \sum_{a,b,b_1,v_1,i}^{i\neq v} \frac{I_{vbb_1v_1}(\Delta_{vb}) I_{v_1aia}(0) I_{ib_1bv}(\Delta_{vb})}{(\epsilon_v-\epsilon_i)^2} \tag{C20}$$

and

$$\Delta E^{(3\mathrm{I})3\mathrm{e,red1}}_{v,\mathrm{S(VP)EVP}} = -\sum_{a,b,b_1,v_1,i}^{i\neq b} \frac{I_{vbb_1v_1}(\Delta_{vb}) I_{b_1aia}(0) I_{iv_1vb}(\Delta_{vb})}{(\epsilon_b-\epsilon_i)^2} \tag{C21}$$

are not found via the perturbative analysis but are present in the redefined vacuum state approach. They are obtained as the interplay among terms generated from the ladder reducible 1 terms, upon the symmetrization of the energy flow in the loop, and four-electron reducible 1 terms. The former originates from $H_1$ while the latter originates from $F_2$. They look like the four-electron reducible 1 contribution, due to the absence of the $\omega$ integration. According to the gauge invariance of the three-electron S(VP)E subset of the two-photon-exchange corrections, they should be incorporated in the three-electron contribution of the three-photon-exchange corrections. The structure of these terms suggests that they be included in the reducible 1 contribution.

## APPENDIX D: THIRD-ORDER INTERELECTRONIC CORRECTIONS DERIVED BY A PERTURBATIVE TREATMENT: THE FOUR-ELECTRON SUBSET

One perturbs the S(VP)E three-electron expressions (14) and (15) according to Eqs. (33)–(36) and finds, under the replacement (37), three different types of four-electron contributions: irreducible (irr), reducible 1 (red1), and reducible 2 (red2). They are displayed below and are further separated into S[V(VP)P]E and S(VP)VP subsets. This separation relies on the redefined vacuum state analysis and its comparison with the perturbative one.

### 1. Irreducible terms

The four-electron irreducible contribution is found to be

$$\Delta E^{(3\mathrm{I})4\mathrm{e,irr}}_{v,\mathrm{S(VP)EVP}} = -\sum_{a,b,c,i,j}^{j\neq v,(i,c)\neq(v,b)} \left(\frac{I_{avaj}(0)[I_{jbci}(\Delta_{vc}) I_{civb}(\Delta_{vc}) + I_{jbic}(\Delta_{cb}) I_{icvb}(\Delta_{cb})]}{(\epsilon_v+\epsilon_b-\epsilon_c-\epsilon_i)(\epsilon_v-\epsilon_j)} + \frac{[I_{cijb}(\Delta_{vc}) I_{vbci}(\Delta_{vc}) + I_{vbic}(\Delta_{cb}) I_{icjb}(\Delta_{cb})] I_{java}(0)}{(\epsilon_v+\epsilon_b-\epsilon_c-\epsilon_i)(\epsilon_v-\epsilon_j)}\right)$$

$$
\begin{aligned}
&- \sum_{a,b,c,i,j}^{j\neq v} \frac{I_{avaj}(0)I_{jicb}(\Delta_{vc})I_{cbvi}(\Delta_{vc}) + I_{vicb}(\Delta_{vc})I_{cbji}(\Delta_{vc})I_{java}(0)}{(\epsilon_b+\epsilon_c-\epsilon_v-\epsilon_i)(\epsilon_v-\epsilon_j)} \\
&- \sum_{a,b,c,i,j}^{j\neq c} \frac{I_{vijb}(\Delta_{vc})I_{jaca}(0)I_{cbvi}(\Delta_{vc}) + I_{vicb}(\Delta_{vc})I_{acaj}(0)I_{jbvi}(\Delta_{vc})}{(\epsilon_b+\epsilon_c-\epsilon_v-\epsilon_i)(\epsilon_c-\epsilon_j)} \\
&- \sum_{a,b,c,i,j}^{j\neq c,(i,c)\neq(v,b)} \frac{I_{acaj}(0)I_{vbci}(\Delta_{vc})I_{jivb}(\Delta_{vc}) + I_{vbji}(\Delta_{vc})I_{civb}(\Delta_{vc})I_{jaca}(0)}{(\epsilon_v+\epsilon_b-\epsilon_c-\epsilon_i)(\epsilon_c-\epsilon_j)} \\
&- \sum_{i,j} \frac{I_{vicb}(\Delta_{vc})I_{iaja}(0)I_{cbvj}(\Delta_{vc})}{(\epsilon_b+\epsilon_c-\epsilon_v-\epsilon_i)(\epsilon_b+\epsilon_c-\epsilon_v-\epsilon_j)}
\end{aligned} \tag{D1}
$$

for the S(VP)EVP subset and

$$
\begin{aligned}
\Delta E^{(3\mathrm{I})4\mathrm{e,irr}}_{v,\mathrm{S[V(VP)P]E}} = &- \sum_{a,b,c,i,j}^{j\neq b,(i,c)\neq(v,b)} \left( \frac{I_{abaj}(0)[I_{vjci}(\Delta_{vc})I_{civb}(\Delta_{vc}) + I_{vjic}(\Delta_{cb})I_{icvb}(\Delta_{cb})]}{(\epsilon_v+\epsilon_b-\epsilon_c-\epsilon_i)(\epsilon_b-\epsilon_j)} \right. \\
&\left. + \frac{[I_{civj}(\Delta_{vc})I_{vbci}(\Delta_{vc}) + I_{vbic}(\Delta_{cb})I_{icvj}(\Delta_{cb})]I_{jaba}(0)}{(\epsilon_v+\epsilon_b-\epsilon_c-\epsilon_i)(\epsilon_b-\epsilon_j)} \right) \\
&- \sum_{a,b,c,i,j}^{j\neq b} \frac{I_{vicj}(\Delta_{vc})I_{jaba}(0)I_{cbvi}(\Delta_{vc}) + I_{vicb}(\Delta_{vc})I_{abaj}(0)I_{cjvi}(\Delta_{vc})}{(\epsilon_b+\epsilon_c-\epsilon_v-\epsilon_i)(\epsilon_b-\epsilon_j)} \\
&- \sum_{a,b,c,i,j}^{(i,c)\neq(v,b),(j,c)\neq(v,b)} \frac{I_{vbci}(\Delta_{vc})I_{iaja}(0)I_{cjvb}(\Delta_{vc}) + I_{vbic}(\Delta_{cb})I_{iaja}(0)I_{jcvb}(\Delta_{cb})}{(\epsilon_v+\epsilon_b-\epsilon_c-\epsilon_i)(\epsilon_v+\epsilon_b-\epsilon_c-\epsilon_j)} \\
&- \sum_{a,b,c,i,j}^{j\neq c,(i,c)\neq(v,b)} \frac{I_{vbij}(\Delta_{cb})I_{icvb}(\Delta_{cb})I_{jaca}(0) + +I_{acaj}(0)I_{vbic}(\Delta_{cb})I_{ijvb}(\Delta_{cb})}{(\epsilon_v+\epsilon_b-\epsilon_c-\epsilon_i)(\epsilon_c-\epsilon_j)}
\end{aligned} \tag{D2}
$$

for the S[V(VP)P]E one.

### 2. Reducible 1 terms

The reducible 1 contribution is also split into S(VP)EVP and S[V(VP)P]E subsets, respectively, and can be cast in the form

$$
\begin{aligned}
\Delta E^{(3\mathrm{I})4\mathrm{e,red1}}_{v,\mathrm{S(VP)EVP}} = &- \sum_{a,b,b_1,v_1,i}^{i\neq b} \frac{I_{vbb_1v_1}(\Delta_{vb})I_{ab_1ai}(0)I'_{iv_1vb}(\Delta_{vb}) + I_{abai}(0)I_{vib_1v_1}(\Delta_{vb})I'_{b_1v_1vb}(\Delta_{vb})}{(\epsilon_b-\epsilon_i)} \\
&- \sum_{a,b,b_1,v_1,i}^{i\neq v} \frac{I_{vbb_1i}(\Delta_{vb})I_{iav_1a}(0)I'_{b_1v_1vb}(\Delta_{vb}) + I_{vbb_1v_1}(\Delta_{vb})I'_{b_1v_1ib}(\Delta_{vb})I_{iava}(0)}{(\epsilon_v-\epsilon_i)} \\
&- \sum_{a,b,c,v_1,i}^{(i,c)\neq(v,b)} \frac{[I_{vbci}(\Delta_{vc})I'_{civb}(\Delta_{vc}) + I'_{vbci}(\Delta_{vc})I_{civb}(\Delta_{vc})]I_{v_1av_1a}(0)}{(\epsilon_v+\epsilon_b-\epsilon_c-\epsilon_i)} \\
&+ \sum_{a,b,c,c_1,i}^{(i,c)\neq(v,b)} \frac{[I_{vbci}(\Delta_{vc})I'_{civb}(\Delta_{vc}) + I'_{vbci}(\Delta_{vc})I_{civb}(\Delta_{vc})]I_{c_1ac_1a}(0)}{(\epsilon_v+\epsilon_b-\epsilon_c-\epsilon_i)} \\
&- \sum_{a,b,c,v_1,i} \frac{[I_{vicb}(\Delta_{vc})I'_{cbvi}(\Delta_{vc}) + I'_{vicb}(\Delta_{vc})I_{cbvi}(\Delta_{vc})]I_{v_1av_1a}(0)}{(\epsilon_b+\epsilon_c-\epsilon_v-\epsilon_i)} \\
&+ \sum_{a,b,c,c_1,i} \frac{[I_{vicb}(\Delta_{vc})I'_{cbvi}(\Delta_{vc}) + I'_{vicb}(\Delta_{vc})I_{cbvi}(\Delta_{vc})]I_{c_1ac_1a}(0)}{(\epsilon_b+\epsilon_c-\epsilon_v-\epsilon_i)}
\end{aligned}
$$

$$+\sum_{a,b,c,v_1,i}^{(i,c)\neq(v,b)}\frac{I_{v_1av_1a}(0)[I_{vbci}(\Delta_{vc})I_{civb}(\Delta_{vc})+I_{vbic}(\Delta_{cb})I_{icvb}(\Delta_{cb})]}{(\epsilon_v+\epsilon_b-\epsilon_c-\epsilon_i)^2}-\sum_{a,b,c,v_1,i}\frac{I_{v_1av_1a}(0)I_{vicb}(\Delta_{vc})I_{cbvi}(\Delta_{vc})}{(\epsilon_b+\epsilon_c-\epsilon_v-\epsilon_i)^2}$$

$$+\sum_{a,b,c,c_1,i}\frac{I_{c_1ac_1a}(0)I_{vicb}(\Delta_{vc})I_{cbvi}(\Delta_{vc})}{(\epsilon_b+\epsilon_c-\epsilon_v-\epsilon_i)^2}-\sum_{a,b,c,c_1,i}^{(i,c)\neq(v,b)}\frac{I_{c_1ac_1a}(0)I_{vbci}(\Delta_{vc})I_{civb}(\Delta_{vc})}{(\epsilon_v+\epsilon_b-\epsilon_c-\epsilon_i)^2} \tag{D3}$$

and

$$\begin{aligned}\Delta E^{(3I)4e,red1}_{v,S[V(VP)P]E}=&-\sum_{a,b,b_1,v_1,i}^{i\neq v}\frac{I_{avai}(0)I_{ibb_1v_1}(\Delta_{vb})I'_{b_1v_1vb}(\Delta_{vb})+I_{vbb_1v_1}(\Delta_{vb})I_{av_1ai}(0)I'_{b_1ivb}(\Delta_{vb})}{(\epsilon_v-\epsilon_i)}\\&-\sum_{a,b,b_1,v_1,i}^{i\neq b}\frac{I_{vbb_1v_1}(\Delta_{vb})I'_{b_1v_1vi}(\Delta_{vb})I_{iaba}(0)+I_{vbiv_1}(\Delta_{vb})I_{iab_1a}(0)I'_{b_1v_1vb}(\Delta_{vb})}{(\epsilon_b-\epsilon_i)}\\&-\sum_{a,b,c,c_1,i}^{(i,c)\neq(v,b)}\frac{[I_{vbic}(\Delta_{cb})I'_{icvb}(\Delta_{cb})+I'_{vbic}(\Delta_{cb})I_{icvb}(\Delta_{cb})]I_{c_1ac_1}(0)}{(\epsilon_v+\epsilon_b-\epsilon_c-\epsilon_i)}\\&+\sum_{a,b,c,b_1,i}^{(i,c)\neq(v,b)}\frac{[I_{vbic}(\Delta_{cb})I'_{icvb}(\Delta_{cb})+I'_{vbic}(\Delta_{cb})I_{icvb}(\Delta_{cb})]I_{b_1ab_1a}(0)}{(\epsilon_v+\epsilon_b-\epsilon_c-\epsilon_i)}\\&+\sum_{a,b,c,b_1,i}^{(i,c)\neq(v,b)}\frac{I_{b_1ab_1a}(0)[I_{vbci}(\Delta_{vc})I_{civb}(\Delta_{vc})+I_{vbic}(\Delta_{cb})I_{icvb}(\Delta_{cb})]}{(\epsilon_v+\epsilon_b-\epsilon_c-\epsilon_i)^2}\\&+\sum_{a,b,c,b_1,i}\frac{I_{b_1ab_1a}(0)I_{vicb}(\Delta_{vc})I_{cbvi}(\Delta_{vc})}{(\epsilon_b+\epsilon_c-\epsilon_v-\epsilon_i)^2}-\sum_{a,b,c,c_1,i}^{(i,c)\neq(v,b)}\frac{I_{c_1ac_1a}(0)I_{vbic}(\Delta_{cb})I_{icvb}(\Delta_{cb})}{(\epsilon_v+\epsilon_b-\epsilon_c-\epsilon_i)^2}.\end{aligned} \tag{D4}$$

### 3. Reducible 2 terms

Each of the inspected subsets participates equally in the reducible 2 contribution. One finds

$$\begin{aligned}\Delta E^{(3I)4e,red2}_{v,S(VP)EVP}=&-\frac{1}{2}\sum_{a,b,b_1,v_1,v_2}\left[I_{vbb_1v_1}(\Delta_{vb})I''_{b_1v_1vb}(\Delta_{vb})+I'_{vbb_1v_1}(\Delta_{vb})I'_{b_1v_1vb}\right]I_{v_2av_2a}(0)\\&+\frac{1}{2}\sum_{a,b,b_1,b_2,v_1}\left[I_{vbb_1v_1}(\Delta_{vb})I''_{b_1v_1vb}(\Delta_{vb})+I'_{vbb_1v_1}(\Delta_{vb})I'_{b_1v_1vb}\right]I_{b_2ab_2a}(0),\end{aligned} \tag{D5}$$

originating from the $H$ diagrams, and

$$\begin{aligned}\Delta E^{(3I)4e,red2}_{v,S[V(VP)P]E}=&-\frac{1}{2}\sum_{a,b,b_1,v_1,v_2}\left[I_{vbb_1v_1}(\Delta_{vb})I''_{b_1v_1vb}(\Delta_{vb})+I'_{vbb_1v_1}(\Delta_{vb})I'_{b_1v_1vb}\right]I_{v_2av_2a}(0)\\&+\frac{1}{2}\sum_{a,b,b_1,b_2,v_1}\left[I_{vbb_1v_1}(\Delta_{vb})I''_{b_1v_1vb}(\Delta_{vb})+I'_{vbb_1v_1}(\Delta_{vb})I'_{b_1v_1vb}\right]I_{b_2ab_2a}(0)\end{aligned} \tag{D6}$$

for the $F$ diagrams.

## APPENDIX E: SYMMETRY ARGUMENT FOR VANISHING LADDER REDUCIBLE 2 TERMS

The cancellation of the $1/\mu$ IR divergence in ladder reducible 2 terms was shown in Table I. This was achieved by searching for a compensating term within the subset of the investigated term. A symmetry argument might also rule out this issue at the individual Feynman diagram level, without the need of a term to absorb its divergence. The naive way to argue would be as follows. Recall that in the Feynman gauge, $I(\omega)$ is a symmetric operator. Therefore, when the IR divergence is met in the ladder reducible 2 term, one faces a symmetric numerator divided by an antisymmetric denominator integrated over a symmetric interval. It vanishes due to parity consideration. However, the problem is that the $i\varepsilon$ prescription spoils the antisymmetric behavior

of the denominator. Hence, a Wick rotation is applied and the expression is

$$\begin{aligned}\frac{i}{2\pi}\int_{-\infty}^{\infty} d\omega \frac{I(\omega)I(\omega)I(0)}{(-\omega+i\varepsilon)^3} &= \frac{-I(0)}{2\pi}\mathcal{P}\int_0^{i\infty} d\omega_E \frac{I(-i\omega_E)I(-i\omega_E)-I(i\omega_E)I(i\omega_E)}{(i\omega_E)^3}\\ &\propto \frac{-i}{2\pi}I(0)\mathcal{P}\int_0^{i\infty} d\omega_E \frac{2\sinh\omega_E R}{\omega_E^3}\\ &\overset{\text{Bl'H}}{=} \frac{-iR}{3\pi}I(0)\mathcal{P}\int_0^{i\infty} d\omega_E \frac{\cosh\omega_E R}{\omega_E^2}\\ &\overset{\text{Taylor}}{\approx} \frac{-iR}{3\pi}I(0)\mathcal{P}\int_0^{i\infty} d\omega_E \left(\frac{1}{\omega_E^2}+\frac{1}{2!}R^2\right).\end{aligned} \tag{E1}$$

Only the principal value is considered since the third-order pole does not contribution to the pole term. One can take the exponential terms of the interelectronic operators out and rephrase them as a hyperbolic sine. Then the Bernoulli-l'Hôpital rule is applied once and the hyperbolic cosine is Taylor expanded, as the interest lies in the low-energy limit. Here $R$ stands for $R = r_{12} + r_{34}$. An interesting feature is seen at this point; it leads to a pure imaginary end result. Furthermore, one retrieves the $1/\mu$ divergent behavior encountered previously. The imaginary contribution to the energy, the decay rate, accounts for the possible instability of the excited states. Since the interest lies in the energy level and not its lifetime, one can neglect it. For completeness, if the ground state is under consideration, it obviously features no instabilities.


[1] X. Fan, T. G. Myers, B. A. D. Sukra, and G. Gabrielse, Phys. Rev. Lett. **130**, 071801 (2023).

[2] T. Sailer, V. Debierre, Z. Harman, F. Heiße, C. König, J. Morgner, B. Tu, A. V. Volotka, C. H. Keitel, K. Blaum *et al.*, Nature (London) **606**, 479 (2022).

[3] M. G. Kozlov, M. S. Safronova, J. R. Crespo López-Urrutia, and P. O. Schmidt, Rev. Mod. Phys. **90**, 045005 (2018).

[4] P. Indelicato, J. Phys. B **52**, 232001 (2019).

[5] A. Gumberidze, T. Stöhlker, D. Banaś, K. Beckert, P. Beller, H. F. Beyer, F. Bosch, S. Hagmann, C. Kozhuharov, D. Liesen *et al.*, Phys. Rev. Lett. **94**, 223001 (2005).

[6] V. A. Yerokhin, P. Indelicato, and V. M. Shabaev, Phys. Rev. Lett. **91**, 073001 (2003).

[7] T. Gassner, M. Trassinelli, R. Heß, U. Spillmann, D. Banaś, K.-H. Blumenhagen, F. Bosch, C. Brandau, W. Chen, C. Dimopoulou *et al.*, New J. Phys. **20**, 073033 (2018).

[8] P. Amaro, S. Schlesser, M. Guerra, E.-O. Le Bigot, J.-M. Isac, P. Travers, J. P. Santos, C. I. Szabo, A. Gumberidze, and P. Indelicato, Phys. Rev. Lett. **109**, 043005 (2012).

[9] S. W. Epp, R. Steinbrügge, S. Bernitt, J. K. Rudolph, C. Beilmann, H. Bekker, A. Müller, O. O. Versolato, H.-C. Wille, H. Yavaş, J. Ullrich, and J. R. Crespo López-Urrutia, Phys. Rev. A **92**, 020502(R) (2015).

[10] C. Brandau, C. Kozhuharov, A. Müller, W. Shi, S. Shippers, T. Bartsch, S. Böhm, C. Böhme, A. Hoffknecht, H. Knopp, N. Grun, W. Sheid, T. Steih, F. Bosch, B. Franzke, P. H. Mokler, F. Nolden, M. Steck, T. Stohlker, and Z. Stachura, Phys. Rev. Lett. **91**, 073202 (2003).

[11] P. Beiersdorfer, H. Chen, D. B. Thorn, and E. Träbert, Phys. Rev. Lett. **95**, 233003 (2005).

[12] D. Bernhardt, C. Brandau, Z. Harman, C. Kozhuharov, S. Böhm, F. Bosch, S. Fritzsche, J. Jacobi, S. Kieslich, H. Knopp *et al.*, Phys. Rev. A **91**, 012710 (2015).

[13] D. Bernhardt, C. Brandau, Z. Harman, C. Kozhuharov, S. Böhm, F. Bosch, S. Fritzsche, J. Jacobi, S. Kieslich, H. Knopp *et al.*, J. Phys. B **48**, 144008 (2015).

[14] I. Draganić, J. R. Crespo López-Urrutia, R. DuBois, S. Fritzsche, V. M. Shabaev, R. S. Orts, I. I. Tupitsyn, Y. Zou, and J. Ullrich, Phys. Rev. Lett. **91**, 183001 (2003).

[15] V. Mäckel, R. Klawitter, G. Brenner, J. R. Crespo López-Urrutia, and J. Ullrich, Phys. Rev. Lett. **107**, 143002 (2011).

[16] Q. Lu, C. L. Yan, G. Q. Xu, N. Fu, Y. Yang, Y. Zou, A. V. Volotka, J. Xiao, N. Nakamura, and R. Hutton, Phys. Rev. A **102**, 042817 (2020).

[17] G. O'Neil, S. Sanders, P. Szypryt, Dipti, A. Gall, Y. Yang, S. M. Brewer, R. Doriese, J. Fowler, A. Naing *et al.*, Phys. Rev. A **102**, 032803 (2020).

[18] M. H. Chen, K. T. Cheng, P. Beiersdorfer, and J. Sapirstein, Phys. Rev. A **68**, 022507 (2003).

[19] P. Beiersdorfer, A. L. Osterheld, J. H. Scofield, J. R. Crespo López-Urrutia, and K. Widmann, Phys. Rev. Lett. **80**, 3022 (1998).

[20] S. A. Blundell, P. J. Mohr, W. R. Johnson, and J. Sapirstein, Phys. Rev. A **48**, 2615 (1993).

[21] J. Sapirstein and K. T. Cheng, Phys. Rev. A **91**, 062508 (2015).

[22] V. M. Shabaev and I. G. Fokeeva, Phys. Rev. A **49**, 4489 (1994).

[23] V. M. Shabaev, Phys. Rep. **356**, 119 (2002).

[24] R. N. Soguel, A. V. Volotka, E. V. Tryapitsyna, D. A. Glazov, V. P. Kosheleva, and S. Fritzsche, Phys. Rev. A **103**, 042818 (2021).

[25] R. N. Soguel, A. V. Volotka, and S. Fritzsche, Phys. Rev. A **106**, 012802 (2022).

[26] A. V. Volotka, D. A. Glazov, V. M. Shabaev, I. I. Tupitsyn, and G. Plunien, Phys. Rev. Lett. **103**, 033005 (2009).

[27] D. A. Glazov, A. V. Volotka, V. M. Shabaev, I. I. Tupitsyn, and G. Plunien, Phys. Rev. A **81**, 062112 (2010).

[28] A. V. Volotka, D. A. Glazov, O. V. Andreev, V. M. Shabaev, I. I. Tupitsyn, and G. Plunien, Phys. Rev. Lett. **108**, 073001 (2012).

[29] A. V. Volotka, D. A. Glazov, V. M. Shabaev, I. I. Tupitsyn, and G. Plunien, Phys. Rev. Lett. **112**, 253004 (2014).
[30] D. A. Glazov, F. Köhler-Langes, A. V. Volotka, K. Blaum, F. Heiße, G. Plunien, W. Quint, S. Rau, V. M. Shabaev, S. Sturm *et al.*, Phys. Rev. Lett. **123**, 173001 (2019).
[31] V. P. Kosheleva, A. V. Volotka, D. A. Glazov, and S. Fritzsche, Phys. Rev. Res. **2**, 013364 (2020).
[32] A. V. Malyshev, A. V. Volotka, D. A. Glazov, I. I. Tupitsyn, V. M. Shabaev, and G. Plunien, Phys. Rev. A **90**, 062517 (2014).
[33] A. V. Malyshev, A. V. Volotka, D. A. Glazov, I. I. Tupitsyn, V. M. Shabaev, and G. Plunien, Phys. Rev. A **92**, 012514 (2015).
[34] A. V. Malyshev, D. A. Glazov, Y. S. Kozhedub, I. S. Anisimova, M. Y. Kaygorodov, V. M. Shabaev, and I. I. Tupitsyn, Phys. Rev. Lett. **126**, 183001 (2021).
[35] J. Sommerfeldt, V. A. Yerokhin, T. Stöhlker, and A. Surzhykov, Phys. Rev. Lett. **131**, 061601 (2023).
[36] S. Weinberg, *The Quantum Theory of Fields* (Cambridge University Press, Cambridge, 1995), Vol. 1.
[37] W. H. Furry, Phys. Rev. **81**, 115 (1951).
[38] I. Lindgren and J. Morrison, *Atomic Many-Body Theory* (Springer, Berlin, 1985).
[39] W. R. Johnson, *Atomic Structure Theory: Lectures on Atomic Physics* (Springer, Berlin, 2007).
[40] R. N. Soguel, A. V. Volotka, D. A. Glazov, and S. Fritzsche, Symmetry **13**, 1014 (2021).
[41] P. J. Mohr, G. Plunien, and G. Soff, Phys. Rep. **293**, 227 (1998).
[42] I. Lindgren, S. Salomonson, and B. Åsén, Phys. Rep. **389**, 161 (2004).
[43] O. Y. Andreev, L. N. Labzowsky, G. Plunien, and D. A. Solovyev, Phys. Rep. **455**, 135 (2008).
[44] V. A. Yerokhin, P. Indelicato, and V. M. Shabaev, Phys. Rev. Lett. **97**, 253004 (2006).
[45] V. A. Yerokhin, C. H. Keitel, and Z. Harman, Phys. Rev. A **104**, 022814 (2021).
[46] V. A. Yerokhin, K. Pachucki, M. Puchalski, C. H. Keitel, and Z. Harman, Phys. Rev. A **102**, 022815 (2020).
[47] E. H. Wichmann and N. M. Kroll, Phys. Rev. **101**, 843 (1956).
[48] G. Kallen and A. Sabry, Selsk. Mat.—Fys. Medd **29**, 17 (1955).
[49] R. Barbieri, J. Mignaco, and E. Remiddi, Lett. Nuovo Cim. **3**, 588 (1970).
[50] R. Barbieri, J. Mignaco, and E. Remiddi, Nuovo Cim. A **11**, 824 (1972).
[51] R. Barbieri, J. Mignaco, and E. Remiddi, Nuovo Cim. A **11**, 865 (1972).
[52] R. Barbieri and E. Remiddi, Nuovo Cim. A **13**, 99 (1973).
[53] E. A. Uehling, Phys. Rev. **48**, 55 (1935).
[54] V. A. Yerokhin, A. N. Artemyev, V. M. Shabaev, M. M. Sysak, O. M. Zherebtsov, and G. Soff, Phys. Rev. A **64**, 032109 (2001).
[55] I. S. Gradshteyn and I. M. Ryzhik, *Table of Integrals, Series, and Products*, edited by A. Jeffrey and D. Zwillinger (Elsevier, Amsterdam, 2007).
[56] J. Sapirstein and K. T. Cheng, Phys. Rev. A **83**, 012504 (2011).
[57] A. Volotka (private communication) (2023).